



UNIVERSITY OF TWENTE.

Faculty of Water Management and Engineering

Processes and parameters underlying the failure of salt marsh vegetation in different sediments

Michiel van den Berg
M.Sc. Thesis August 2021

Supervisors:

Dr. Ir. B. W. Borsje
Dr. P.W.J.M Willemsen
Dr. Ir. J.T. Dijkstra

Faculty of Engineering technology
Water Engineering and Management
University of Twente
P.O. Box 217
7500 AE Enschede
The Netherlands

Preface

Before you lies the thesis report “The processes and parameters underlying the failure of juvenile pioneer salt marsh vegetation in different sediments”, the basis of which is a flume experiment carried out at Deltares in Delft. This thesis represents the conclusion studies at the University of Twente.

This thesis would not have been possible without the help and support of a number of people. First, I would like express my gratitude to my supervisors for their feedback and support during my research.

Bas Borsje, as my UT supervisor, presented me with the opportunity to work on this project and provided valuable feedback. Pim Willemsen, for his support and counsel as my daily supervisor. He also made fieldwork at the Marconi site possible, which I enjoyed and also gave me some hands-on experience of the salt marsh conditions in the field. Jasper Dijkstra, for his feedback and support as my external supervisor and for giving me the opportunity to carry out the flume experiment at Deltares, which I enjoyed very much and gave me a lot of insight in the practical side of gathering experimental data.

I would also like to thank Floris van Rees for his help during the experiment and feedback on my research and Peter Alberts for his help while conducting the flume experiment.

I also wish to thank Liesje Mommers of the Wageningen University for her correspondence about vegetation growth.

Finally, I would like to thank my family, friends and housemates for their support during my study and this research. Especially my housemates for being fine with me working in our living room when my room became suffocating due to the pandemic.

Michiel van den Berg,
Enschede, August 16, 2021

Abstract

Salt marshes are considered valuable habitats and provide a wide range of ecosystem services, including contributing to coastal protection, stabilising coastlines, carbon storage and providing habitat and marine nursery grounds. Therefore, many projects have attempted to create and restore salt marshes but are often hindered by a lack of thorough understanding of initial vegetation establishment. To determine if vegetation can establish on an intertidal flat, Balke et al. (2011) developed the Windows of Opportunity (WoO) framework. The framework consists of three successive periods or windows, in which certain hydrodynamic conditions can not be exceeded. In the first window, vegetation requires a short disturbance-free period to develop roots (WoO1). This is followed by a period with calm hydrodynamic conditions (WoO2) in which the vegetation's roots can gain more strength and a period in which the high-energy events do not exceed the vegetation limits (WoO3). This thesis aims to determine the conditions under which juvenile pioneer salt marsh vegetation fails and how this knowledge can be applied for the restoration and creation of salt marshes.

An experiment was used to study the above and below ground development of juvenile pioneer salt marsh vegetation in different sediments. The plants were subsequently tested in a wave flume, using irregular waves to examine failure. For this experiment the pioneer salt marsh species "*Salicornia procumbens*" was selected; this species is native to the Dutch coast and often one of the first plants to establish on bare intertidal flats. Four batches of seedlings of different ages were cultivated and tested in defaunated cohesive sediment (mud) and non-cohesive sediment (sand). During the flume experiment the wave height and flow velocity were measured at several locations in the wave flume.

The development of *Salicornia* seedlings aboveground was comparable in sediment of the cohesive and non-cohesive type, although, in cohesive sediment, the plants became more complex in a shorter period. Belowground, the bio morphology of the *Salicornia* seedlings was significantly different. In sand, a complex root system developed with numerous long thin roots, while in cohesive sediment, the roots were

thick and short and the root system relatively simple. This difference was most likely related to the increase in soil strength as a result of the consolidation in cohesive sediment and other sediment properties like nutrient availability. Another consequence of this consolidation and increase in soil strength was that the erosion resistance increased rapidly in recently deposited cohesive sediment.

The irregular waves in the flume stressed the seedlings due to the to-and-fro motion of the plants and erosion as a result of the oscillating flow velocities produced by the waves. Seedlings in cohesive sediment received on average more wave energy over time because of the larger frontal surface area of these seedlings. Moreover, distinct failure mechanisms were observed between the sediment types. In non-cohesive sediment, erosion was the dominant process causing failure, while in cohesive sediment, the to-and-fro motion of the plants that pried out and broke the roots was the dominant process causing failure. Furthermore, the seedlings growing in cohesive sediment could withstand a more extended period of wave loading and more wave energy before failure, compared to seedlings of similar age in sand.

In practice, sediment with higher clay content may result in a higher survival rate of *Salicornia* seedlings on the intertidal flats, especially near the regions with harsher hydrodynamic conditions. *Salicornia* stands enable perennial salt marsh plants to establish on the intertidal flats, for example, by trapping vegetative tillers of these plants. These species are essential for further increasing biodiversity and plant succession on a recently established salt marsh as well as stabilising the soil. This, subsequently, will benefit the ecosystem services like wave attenuation, carbon storage and provides more habitat and marine nursing grounds.

Contents

Preface	iii
Abstract	v
List of Symbols	xi
1 Introduction	1
1.1 Restoration efforts	2
1.2 Physical stressors that influence salt marsh vegetation and failure . .	3
1.3 Erosion and consolidation of sand-mud mixtures	3
1.4 The Windows of Opportunity (WoO) framework	6
1.5 Knowledge gaps	7
1.6 Research objective	9
1.7 Research questions	9
2 Methods	11
2.1 Flume experiment: failure of <i>Salicornia procumbens</i> seedlings	11
2.1.1 Preparation: growing plants and collecting sediment	12
2.1.2 Flume sample preparation	14
2.1.3 Flume tests and measurements	14
2.2 Flume experiment: sediment characteristics of fresh mud	17
2.2.1 Flume sample preparation	17
2.2.2 Flume tests and measurements	17
2.3 Calculation of plant traits	18
2.3.1 Frontal surface area of the aboveground biomass	18
2.3.2 Surface area of the root system	18
2.3.3 Density of fresh <i>Salicornia</i>	19
2.4 Calculation time and received energy in the flume	19
2.4.1 Adjusted time in the flume	19
2.4.2 Energy received by plant and drag force	19
2.5 Forces on the seedlings	21

2.5.1	Calculation of the gravity force and the buoyancy in force balance	21
2.5.2	Root anchorage	22
2.5.3	Dynamic force on seedling, momentum	23
2.6	Bed shear stress	25
2.7	Statistical methods	26
2.7.1	Averages and standard deviation	26
2.7.2	Significance of the difference (T-test)	26
3	Results	29
3.1	Development of sediment over time	29
3.2	Development <i>Salicornia</i> seedlings in different sediments	31
3.2.1	Morphological plant characteristics of the aboveground biomass	31
3.2.2	Morphological plant characteristics of the belowground biomass	35
3.3	Effect of plant traits on failure	37
3.4	Seedlings under irregular waves	40
3.5	The different failure mechanisms observed during the flume experiment	44
3.5.1	Stage 1: initial forces on seedling	46
3.5.2	Stage 2 and stage 3: begin and development scour-hole	47
3.5.3	Stage 4: failure of the plant and behaviour once failed	50
3.6	Thresholds of the failure of <i>Salicornia</i> seedlings	51
3.6.1	Failure thresholds in non-cohesive sediments	51
3.6.2	Failure threshold in cohesive sediments	52
3.7	Expanse of the WoO framework	54
4	Discussion	57
4.1	Methods of the flume experiment and observations	57
4.2	The biophysical plant parameters	59
4.3	Erosion and consolidation of sand-mud mixtures	59
4.3.1	Erosion and sediment transport during short storm events vs longer moderate events	61
4.4	Irregular vs regular waves	62
4.5	Seedling failure	66
4.6	Practical implications	67
4.6.1	Implications for the Windows of Opportunity framework	67
4.6.2	Practical implications for salt marsh restoration and creation	68
5	Conclusions and recommendations	71
5.1	Research question 1	71
5.2	Research question 2	73

5.3 Recommendations for future flume experiments	74
References	75
Appendices	
A Drag coefficients in different flow regimes	83
B Flow velocity field	85
C Calculation of species-specific attachment coefficient (k)	87

List of Symbols

A	Wave amplitude	[m]
$A_{frontal}$	Frontal surface area of a <i>Salicornia</i> seedling	[m ²]
A_r	Root area	[m ²]
C_d	Drag coefficient	[-]
C_u	Sediment cohesion	[Pa]
c_u	Undrained shear strength	[Pa]
c_d	Drained shear strength	[Pa]
c_v	pore water dissipation	[m ² /s]
D_{50}	Median sediment grain size	[m]
E_s	Surface erosion rate	[$\frac{kg}{m^2s}$]
F_a	Root anchorage force	[N]
F_b	Buoyancy force	[N]
F_d	Drag force	[N]
F_g	Gravity force	[N]
H	Wave height	[m]
h	Water depth	[m]
h_v	Height of the vegetation	[m]
h_{adjust}	Plant height compensated for the frontal surface area	[m ²]
j	Species-specific attachment coefficient mass	[-]
k	Species-specific attachment coefficient surface	[-]
k_s	Nikuradse bed roughness	[m]
M_g	Momentum of gravity force	[N/m]
M_r	Dry root mass	[kg]
m_{plant}	Mass of a single <i>Salicornia</i> seedling	[kg]
M_s	Surface erosion parameter	[$\frac{kg}{m^2Pas}$]
N_v	Vegetation density	[-]
Re	Reynold's number	[-]
T	Wave period	[s]
t	Time	[s]
u	Flow velocity	[m/s]

U_b	Maximum flow velocity near the bed	$[m/s]$
V_{plant}	Volume of a plant	$[m^3]$
x	Position in the x direction	$[m]$
y	Position in the x direction	$[m]$
z	the distance from the bed	$[m]$
δ_e	Erosion depth	$[m]$
ν	kinematic viscosity	$[m^2/s]$
\emptyset_{stem}	Stem diameter of a <i>Salicornia</i> seedling	$[m]$
ω	Angular velocity	$[1/s]$
ρ_w	density of water	$[kg/m^3]$
$\rho_{Salicornia}$	Density of fresh <i>Salicornia</i>	$[kg/m^3]$
ρ_{dry}	Density of dry sediment	$[kg/m^3]$
τ_b	Bed shear stress	$[Pa]$
τ_e	Critical bed shear stress	$[Pa]$
$\bar{\tau}_b$	Mean bed shear stress	$[Pa]$
$\bar{\tau}_e$	Mean critical bed shear stress	$[Pa]$
$\hat{\tau}_b$	Turbulent fluctuation of the bed shear stress	$[Pa]$
$\hat{\tau}_e$	Turbulent fluctuation of deviatoric critical bed stress	$[Pa]$

Introduction

In the past decennia, the social and scientific perception of salt marshes experienced a transition (Gedan et al., 2009). Instead of viewing these intertidal wetlands as swampy wastelands used to buffer human impacts along the coast, salt marshes are considered valuable habitats whose worth is generated by a suite of ecosystem services (Gedan et al., 2009). For example, salt marshes contribute to coastal protection by dissipating wave energy, stabilising shorelines and mitigating coastal flooding (Jadhav et al., 2013). Furthermore, the carbon storage performed by salt marshes gains importance with climate change; salt marshes are effective carbon sinks (Gedan et al., 2009). In addition to this, salt marshes also deliver ecosystem services, including support of biodiversity (Adam, 2018) and providing habitat and marine nursery grounds (Mohan et al., 2019; Townend et al., 2011).

More than 40% of the world's population resides near the coasts (Gedan et al., 2009)) and are vulnerable to flooding events and sea-level rise. Climate change will increasingly affect sea-level rise and storm intensity, frequency, and duration in future scenarios. These are key drivers that influence sea level extremes and ocean waves (Church & Gregory, 2019), increasing the risk and magnitude of coastal flooding (JRC PESETA II project, 2009). This increasing flood risk combined with a growing coastal population, is the reason why salt marshes are increasingly valued for their function of coastal protection. Contradictorily, due to numerous stresses, the amount of natural salt marsh area has diminished significantly (Rozas et al., 2016; William, 2019). Stresses like land reclamation, coastal squeeze, alterations in wetland drainage and sediment inputs have caused the disappearance of half of the salt marshes in the world in the last century (Mitsch & Gosselink, 2007; Nicholls et al., 1999; William, 2019).

1.1 Restoration efforts

The reevaluation of how society perceives salt marshes and how they can be utilised for coastal protection, led to growing interest in conserving and recreating these tidal wetlands, resulting in worldwide efforts to restore salt marshes (Sun et al., 2010). Projects in China (Sun et al., 2010), The United States (Faber & Phyllis, 2001; Rozas et al., 2016) and Europe (Wolters et al., 2005) have actively tried to restore salt marshes, with mixed success. The process of recreating salt marshes is often not simple and the effect of certain interventions is often uncertain. For example, active planting does not necessarily lead to the successful establishment of marshes (Cao et al., 2018). In addition, other restoration techniques like brushwood fences or construction of offshore breakwaters to limit erosion, can be expensive and labour-intensive or require constant monitoring (Nottage & Robertson, 2005). Therefore, studying and quantifying the parameters that influence successful salt marsh establishment can improve the effectiveness of some restoration efforts.

For restoring salt marshes, it is essential to understand how the transition of a barren mud or sandflat to a biodiverse salt marsh is dictated. Pioneer salt marsh species are key for this transition. The pioneer species of the genus *Salicornia* L., are frequently the first vascular plants colonising the low salt marsh (Davy et al., 2001) and enable other species to colonise a bare intertidal flat. *Salicornia* is therefore essential for successful salt marsh establishment. So it is imperative to know the vulnerabilities of this pioneer plants species in the corresponding lifecycle stages, to prevent failure due to physical stress. *Salicornia* is an annual halophyte that forms sparse vegetation patches consisting of stiff shoots (Bouma et al., 2013). Annual plants are plant species that conclude their life cycle within one growing season. After completion of its life cycle, from germination to the production of seeds, the plant perishes and the cycle starts over again. So every year an entirely new population of *Salicornia* plants is built up (Beeftink, 1985). The life cycle of *Salicornia* can be divided in several phases. Each phase presents its own vulnerabilities.

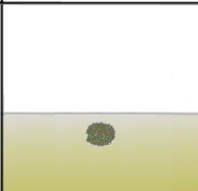
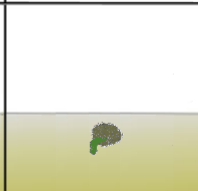
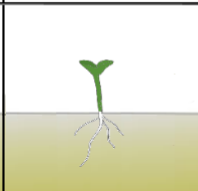
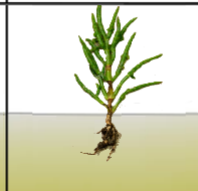

The different growth phases of <i>Salicornia Procumbens</i>	Seed Phase	Germination phase	Seedling phase	Adult phase	Flowering and seed production phase
					

Figure 1.1: Growth phases of *Salicornia procumbens*

1.2 Physical stressors that influence salt marsh vegetation and failure

Many factors determine the success of salt marsh creation, and many involved processes are poorly understood. Only a handful of studies have focused on physical disturbance mechanisms in the salt marsh pioneer zone (Balke, 2013; Cao et al., 2018; Schoutens et al., 2021). In recent years the focus on salt marsh vegetation has elevated and several research papers have been written that pertain to salt marsh pioneer vegetation. These studies focus primarily on the germination and seedling phase of the vegetation because these phases are critical for salt marsh establishment; pioneer vegetation like *Salicornia* is most vulnerable in these phases. Many physical stressors influence juvenile salt marsh vegetation development. These parameters include bed level change, temperature, nutrient availability, sedimentation, inundation free period, inundation frequency and hydrodynamic energy (Cao et al., 2018; Friess et al., 2012; Hendriks, 2020; Houwing, 2000; van Regteren et al., 2020; Willemsen et al., 2018).

On salt marshes, there are also many processes that lead to seedling failure. Multiple environmental variables such as oxygen limitation, bioturbation and salt stress may cause a seedling to fail. This study, however, focuses primarily on mechanical failure as a result of wave action. Mechanical failure of individual seedlings depends on the equilibrium between the vectorial sum of the buoyancy, together with drag forces of the waves on the aboveground biomass and the resistance due to root anchoring (Edmaier et al., 2011). If this equilibrium is unbalanced, for example due to erosion, the seedlings will topple or flush away completely and will be deemed to have failed.

1.3 Erosion and consolidation of sand-mud mixtures

Intertidal sediments in estuaries generally consist of a mixture of sand and mud; both fractions mutually influence the soil mechanical and therefore, the morphological behaviour of sand-mud mixtures (Jacobs, 2011). Different geotechnical failure mechanisms are presented in the research of Jacobs (2011), that characterises different erosion modes as a function of flow-induced stresses and soil mechanical parameters. Bed stability is generally related to gravitational, adhesive or cohesive forces, whereas in geotechnical engineering, the (un)drained sediment strength is applied (Jacobs, 2011). The drained and undrained sediment strength may differ by orders of magnitude. Erosion modes are therefore divided between drained (floc

and surface erosion) and undrained failure mechanisms (mass erosion). Drained refers to cohesive and adhesive forces, whereas undrained refers to apparent cohesion.

A stable bed occurs when turbulent stress fluctuations (τ_b) do not exceed the drained strength of the bed (c_d). When these fluctuations exceed c_d , flocs are locally eroded (i.e. floc erosion). Surface erosion occurs when $\bar{\tau}_b$ is larger than c_d , but smaller than the undrained strength (c_u). Finally, mass erosion occurs when $\hat{\tau}_b$ exceeds c_u . Floc and surface erosion may co-occur (Jacobs, 2011).

Floc and surface erosion are expected to govern the morphological behaviour of estuaries and are susceptible to biological and physicochemical influences. Floc erosion concerns the removal of individual flocs due to turbulent peak stresses exceeding the drained bed strength. Surface erosion is less dependent on the stochastic character of the flow. The research of Jacobs (2011) derived a formula for the surface erosion (equation 1.1 and equation 1.2), assuming that failure of the bed occurs at the critical state. E_s is the surface erosion rate and M_s the surface erosion parameter. M_s is a function of the coefficient of pore water dissipation and the undrained strength.

$$E_s = M_s(\tau_b - \tau_e) \text{ for } \tau_b > \tau_e \quad (1.1)$$

$$M_s = \frac{c_v \rho_{dry}}{\delta_e c_u} \quad (1.2)$$

where:

E_s	the surface erosion rate ($kg * m^{-2} s^{-1}$)
M_s	the surface erosion parameter ($kg * m^{-2} s^{-1} Pa^{-1}$)
τ_b	the bed shear stress (Pa)
τ_e	the critical bed shear stress (Pa)
c_u	the undrained shear strength (Pa)
c_v	the pore water dissipation (m^2/s)
δ_e	the erosion depth (m)
ρ_{dry}	the density of dry sediment (kg/m^3)

The undrained shear strength is directly related to the consolidation degree of the sediment and increases over time (Germaine et al., 1998). Therefore, the consolidation process is an essential factor when calculating the surface erosion parameter (equation 1.2). The consolidation process is not linear, and divided into several phases (Figure 1.2). During the first phase of consolidation, the primary consolida-

tion phase, a slow-building up of contact forces (grain stresses), is accompanied by relatively large strains, and the pore water is driven out (van Rijn & Barth, 2018). Most soils continue to compress after the primary consolidation phase due to creep deformation of the soil structure. This phenomenon is called secondary consolidation (Germaine et al., 1998). The settling and consolidation processes are essentially vertical processes with a downward movement of sediments and upward movement of expelled pore water (van Rijn & Barth, 2018).

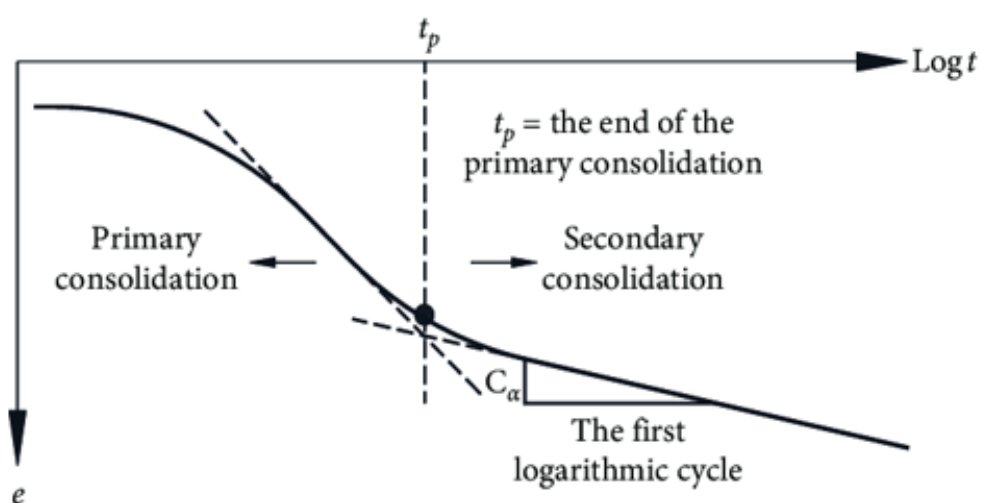


Figure 1.2: Diagram of the division of the primary consolidation and the secondary consolidation (Wang et al., 2020)

The research of Khan et al. (2014) also noted that erosion resistance of cohesive sediment increased with decreasing water content and compaction of the material. In addition to this, Kothyari et al. (2014) showed that erosion rate decreases with the increase in clay content of cohesive sediment.

Therefore, the clay content and soil strength of the sediment will affect the formation of a depression around a seedling. This depression around a seedling can disrupt the equilibrium between uprooting forces and the resistance due to root anchoring. The term for the formation of an erosion depression around a plant is scouring or self-scouring. Scouring is the process in which the presence of vegetation generates vortices that locally change the bottom stress induced erosion around the plant (Bouma et al., 2009; Friess et al., 2012). Another process for the formation of a depression around a plant is local sediment deformation. Sediment deformation is the process in which the to-and-fro motion of the plant due to wave action creates a narrow cavity around the base of the plant.

1.4 The Windows of Opportunity (WoO) framework

To determine whether hydrodynamic conditions permit salt marsh establishment, the Windows of Opportunity (WoO) framework can be used. This framework, consisting of three subsequent windows, was developed by Balke et al. (2011), and initially intended for the establishment of mangrove seedlings. Seeds that start germinating, require a disturbance-free period to grow roots and gain some anchorage to the bed and not be flushed away instantly (WoO1). This disturbance-free period needs to be followed by a period with calm hydrodynamic conditions (WoO2) in which the seedlings can grow stronger and increase root anchorage. In the next window (WoO3), the plants are mature and well-rooted. In this period, high-energy events should not exceed the uprooting limits of the vegetation.

Recently the framework was adapted and applied to evaluate salt marsh establishment (Cao et al., 2018; Hu et al., 2015; D. W. Poppema et al., 2019) (Figure 1.3). It states that juvenile salt marsh vegetation can establish when the local conditions on the intertidal flats remain below the thresholds of the subsequent windows of opportunity. In the research of Hu et al. (2015), the WoO framework was defined in terms of critical bed shear stress (BSS), which was used as a proxy for erosion, where BSS, only expresses the conditions at a specific point in time. The effect of sedimentation and erosion on the seedlings accumulates over time. So erosion and sedimentation can influence the seedlings without the need for strong BSS peaks. To improve the framework D. W. Poppema et al. (2019) used bed level change instead of BSS to simulate erosion. This change enables the WoO framework to take the effects of both moderate conditions and extreme events into account.

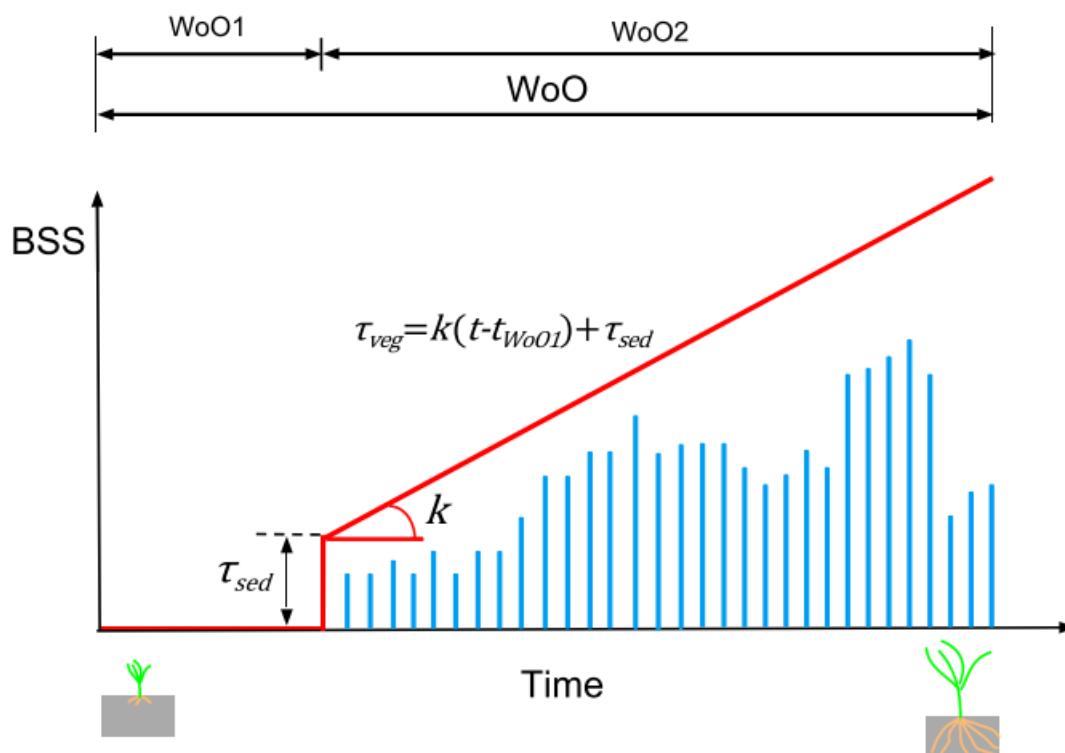


Figure 1.3: An illustration of the WoO framework, showing a scenario with successful establishment. The bed shear stress (blue lines) always remains under the time-dependent critical bed shear stress (red line) (Hu et al., 2015)

1.5 Knowledge gaps

Most studies that explore the restoration of salt marshes look into salt marsh establishment on a macro level (Gedan et al., 2009; Lo et al., 2017; Spencer et al., 2016; van der Wal & Herman, 2012; Yeager et al., 2009). Only a handful of experiments have been conducted to investigate the processes that induce failure of individual seedlings, so the available data on how individual seedlings fail and influence salt marsh establishment is minimal (Cao et al., 2019; D. W. Poppema et al., 2019; Silinski et al., 2016).

The adaptation of the Windows of Opportunity framework is a result of the most recent research into the establishment of salt marsh vegetation. However, the effect of sediment type on the WoO framework, especially in WoO2, is not yet explored in depth. Almost all previous research was done with exclusively sandy sediments (Cao et al., 2018; Edmaier et al., 2011; D. W. Poppema et al., 2019; Silinski et al., 2016). In reality, salt marshes consist of a wide range of sediment types and sediment mixture. It is not unconventional for these sediments to have high mud content

and cohesive characteristics (Bradley & Morris, 1990). Research at the Marconi site in Delfzijl already demonstrated that a high clay content in the sediment could positively affect the establishment of salt marsh pioneer vegetation (De Vries et al., 2021; Hendriks, 2020). Investigating the effect of sediment type on the WoO2 window can therefore be imperative to accurately simulate the establishment of a wider variety of salt marshes.

Previous research used monochromatic waves to simulate hydrodynamic conditions present on intertidal flats (Balke et al., 2011; D. W. Poppema et al., 2019). The research of Balke et al. (2011) used currents in addition to waves, but Callaghan et al. (2010) found that waves are dominant over currents as a forcing mechanism. In reality, however, incoming wave trains are not monochromatic. So the hydrodynamic conditions used in these previous studies might not accurately represent the conditions typical for intertidal flats. Therefore, investigating the effect of adopting irregular waves instead of monochromatic waves (which are closer to wave conditions in the field) might be beneficial. Especially because these irregular waves might induce different modes of failure in salt marsh vegetation compared to regular waves; for example, breakage of the roots, failure of soil-root cohesion (slipping) and failure of soil cohesion at the edge of the root ball (Schutten et al., 2005).

summarise, three (separate) knowledge gaps in existing literature have been identified:

- The processes that induce failure in individual pioneer salt marsh seedlings are still understudied; only a few studies have looked into the failure of individual seedlings
- The effect of sediment properties, especially of cohesive sediment, on the establishment of salt marsh pioneer vegetation, has not been explored in depth yet
- The effect of irregular waves (in contrast to monochromatic waves) on the establishment of salt marsh pioneer vegetation has not yet been studied

1.6 Research objective

The purpose of this research is to resolve the identified knowledge gaps. To accomplish this, the following research objective is defined:

“To determine a set of biophysical parameters and processes underlying the failure of juvenile pioneer salt marsh vegetation, specifically the effect of sediment properties (cohesive and non-cohesive) and wave characteristics, and use these findings to improve the understanding of salt marsh plant failure”

The set of biophysical parameters that will be studied in this research are the morphological plant traits (plant height, stem diameter, frontal surface area, root length and root thickness), the characteristics of irregular waves (oscillatory flow velocity, flow-induced shear stress) and the sediment properties (cohesive and non-cohesive, consolidation, shear strength and erosion resistance). For this research the salt marsh species *Salicornia procumbens* is used as representative pioneer salt marsh vegetation.

1.7 Research questions

1. *How do plant traits, sediment properties and wave characteristics affect the critical erosion depth and failure of juvenile pioneer salt marsh vegetation species “Salicornia procumbens ”?*
 - a. *How do plant traits affect the critical erosion depth and failure of Salicornia procumbens seedlings?*
 - b. *How do sediment properties (cohesive vs. non-cohesive) affect the plant and plant traits over time of Salicornia procumbens seedlings?*
 - c. *How do sediment properties (cohesive vs. non-cohesive) affect the critical erosion depth and failure of Salicornia procumbens seedlings?*
 - d. *How do irregular wave characteristics affect the critical erosion depth and failure of Salicornia procumbens seedlings?*

This question aims to determine how plant traits, sediment properties, and wave characteristics affect the critical erosion depth and failure of pioneer salt

marsh vegetation. Using the data obtained from the flume experiment, the relationships between these parameters will be examined. The possible biophysical relations that are obtained are then evaluated using statistical methods like the Pearson correlation method and student's T-test.

2. *How can the observations of the flume experiment improve the understanding of salt marsh vegetation failure?*
 - a. *How can the observations of the flume experiment be used to improve the Windows of Opportunity framework for salt marsh establishment?*
 - b. *What are the practical implications of the observations of the flume experiment for restoration of salt marshes?*

This research question aims to expand the WoO framework introduced by Balke et al. (2011) and revised by D. W. Poppema et al. (2019) and explore the practical implications of the observations of the flume experiment. Explicitly effect the influence of sediment properties and wave characteristics on the seedling establishment of *Salicornia* seedlings.

Methods

In this chapter, the methods and practices used to answer the research questions are described. First, the setup and methodology of the flume experiment are presented in sections 2.1 and 2.2. Next, in sections 2.3, 2.4, 2.5 and 2.6, the determination of different plant parameters and wave characteristics are considered. This is followed by section 2.7, where the statistical methods used to evaluate the experiment's findings are explained.

2.1 Flume experiment: failure of *Salicornia procumbens* seedlings

The research of Callaghan et al. (2010) found that for the hydrodynamic forcing on the bottom sediment, the influence of wind-generated waves was dominant compared to tidal- or wind-driven currents. Therefore, a wave flume producing irregular waves was selected for the experiment. The purpose of the flume experiment was to determine the thresholds like critical erosion depth (CED) for the successful establishment of pioneer plants in salt marshes. The CED is defined as the minimum net erosion occurring in a short amount of time that causes a seedling to to (Bouma et al., 2016). Furthermore, the experiment aims to determine the impact of sediment type and wave load over time on the CED. Section 2.1.1 presents the procedure for the preparation of the flume experiment. Section 2.1.2 describes the preparation of the samples before entering the flume, followed by section 2.1.3, which describes the measurement methods used during the experiment.

In this research, *Salicornia procumbens* (Glasswort) was selected for the experiments because it is a pioneer species on mudflats both in the Westerschelde and Wadden Sea. Moreover, the relatively small plant size of *Salicornia* allows flume experiments without the need for scaling and makes manual handling straightforward.

In addition, since *Salicornia* is an annual plant that spreads by producing seeds, good seeds are relatively easy to obtain and they germinate fairly easy in contrast to e.g. *Spartina*, which is a perennial plant that mainly spreads via its root system and is more troublesome to grow from seeds in the limited time available.

2.1.1 Preparation: growing plants and collecting sediment

The *Salicornia procumbens* seeds originated from the salt marshes at Rattekaai in the western part of the Eastern Scheldt and were collected in 2018. The seeds germinated in a climate-controlled environment at room temperature on moist (mildly saline; 7 g NaCl/l) paper towels for seven days. The sediment was obtained from the intertidal mudflats near Zuidgors, Westerschelde. The sediment was defaunated by freezing for ten days and kept in closed buckets until further use. Part of the collected sediment was mixed with fine sand (115 microns, poorly graded; 85 kg sand + 6.5 kg mud) to create a sandy substrate. The Zuidgors sediment consists of 16.8% clay, 60.5% silt and 22.6% sand with a D50 of 18 microns (Malvern Mastersizer analysis).

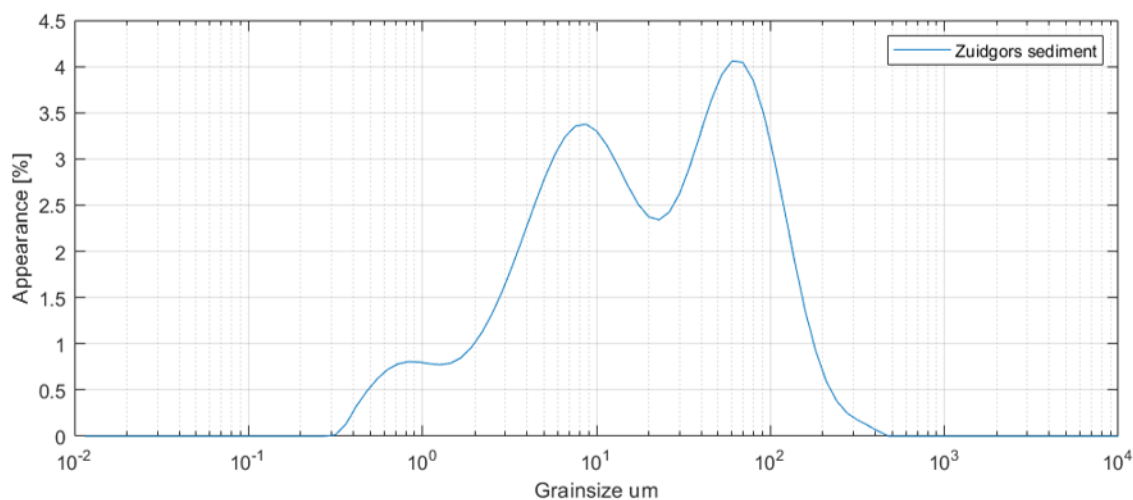


Figure 2.1: Particle size distribution Zuidgors sediment

After the germination process, the seedlings were planted in rectangular boxes filled with homogenised Zuidgors sediment. The moment of planting was considered timestep 0 in the growing process. The moment the plants were placed in the flume was the final timestep. During germination, the seedlings already developed roots and shoots, so the morphological plant characteristics were not zero at the time of placement. Therefore 18 seedling samples were selected and measured before placement in the boxes. The resulting average value for various plant characteris-

Table 2.1: age of the sample batches

Batch	Placement date	time between placement	Relative age to last batch
1	11-8-2020	8	22
2	19-8-2020	6	14
3	25-8-2020	4	8
4	2-9-2020	0	0

tics, like root length, shoot length, root thickness, stem diameter and frontal surface area, were used as starting values for all seedlings at timestep 0. Four batches of boxes with samples were created at four time intervals so tests could be conducted with plants of various ages. The aboveground development of the seedlings was monitored and documented during the growing phase.

The dimensions of the boxes in which the germinated *Salicornia* seedlings were placed were: 60 cm length, 15 cm width, 15 cm internal depth, 17 cm stack height. The length allows placement of plants at 20 cm from either side, which was considered sufficient to avoid plant-induced scour interfering with rim-induced erosion. because of the width of the boxes, no substantial rim-induced erosion was expected. Therefore, two seedlings could be placed at each side of a box (1 cm apart) and grown in situ to avoid losses to impaired seedling growth. So, each box contained four seedlings, at 20 cm from the rim. If all seedlings survived, one individual was eliminated at each side before the flume experiment was initiated to prevent interaction between the seedlings.

Half of the boxes were filled with the original silty Zuidgors sediment and the other half was filled with the mixed sandy sediment. The boxes had a vertically adjustable bottom to raise the sediment to the box rim in case of consolidation. The boxes were irrigated bidaily for 5 min with fresh water without fertiliser and they were not watertight so excess water could drain. The depth of the sediment in the boxes was larger than the foreseen root depth of *Salicornia procumbens*. Furthermore, the seedlings were not protected from the abiotic environment (wind, rain, sun, etc.). The boxes were however protected from biotic factors like foraging animals.

During the growing phase of the experiment, per batch one box of each sediment type was filled with sediment and no seedlings. These boxes were used to determine specific sediment characteristics at different ages, like the shear strength using a shear vane. Each box was sufficiently large so at least two shear measurements could be conducted.

In addition to the samples germinated in a climate-controlled environment and artificially grown in the rectangular boxes, some plants were collected from the field to investigate the difference between artificially grown plants and plants grown in the field. These plants originated from the Marconi project site near Delfzijl. The plants were collected at two sections of the Marconi site with different sediment compositions of the top layer (samples from the section with 5% clay and samples from the section with 50% clay). So during the experiment also the effect of different sediments on the field plants could be examined.

2.1.2 Flume sample preparation

Preceding each run of the flume experiment, each chosen box with samples was prepared and documented. The sediment consolidation in each box was measured at six locations; at the corners and in the middle at both sides. The consolidation was measured using a ruler. These six measurements were used to calculate an overall mean value for the consolidation per box. Next, the dimensions of the above-ground biomass of the seedlings in each box were measured (plant height, stem thickness). The plant height was measured using a ruler and the stem thickness was measured using a calliper. Furthermore, the plants were photographed in front of a white background. The background included a scale, so the frontal surface area of the plants could subsequently be determined using photoshop. Depending on the survival rate of the seedlings during the growing phase of the experiment, the excess of plants in the boxes was removed. This was done using a tensile strength meter to measure the pulling force a plant could withstand. The root length and root thickness of the pulled-out seedlings were measured with a ruler and calliper, respectively. The condition of the root system was noted; this included observations pertaining to the health of the roots, the complexity of the root system and if the roots broke during the pulling process.

In several boxes, the bed level did not align with the top edge of the boxes. Especially the boxes filled with mud exhibited significant consolidation. Therefore, the bed elevation was adjusted to match the top edge of the box before placement in the flume. Furthermore, several boxes displayed a hardened top layer or biofilm. This layer was carefully removed.

2.1.3 Flume tests and measurements

For the flume experiments the Westerscheld flume of Deltares in Delft was used. The flume measures 55 meters in length, has a width of 1 meter and a height of 1.2

meters (Figure 2.2). A double bottom was built into the flume, so the boxes with plants could be lowered into the flume at bed level. This double bottom reduced the initial bottom by 18 cm. The transition zone leading to the double bottom was located 37 meters from the front of the flume and had a slope of 1:50.

For this experiment a water height of 0.5 meters was used in the flume. Waves were generated at one side of the flume, and at the other side, a vertical “cliff” was installed. An Active Reflection Compensation (ARC) system, which eliminates reflecting waves, was activated during the experiment. Several wave conditions were tested and the most suitable wave conditions were determined. The experiment used irregular waves with a period of 2.5 seconds and an amplification factor of 0.5 to 0.8 (table 2.2).

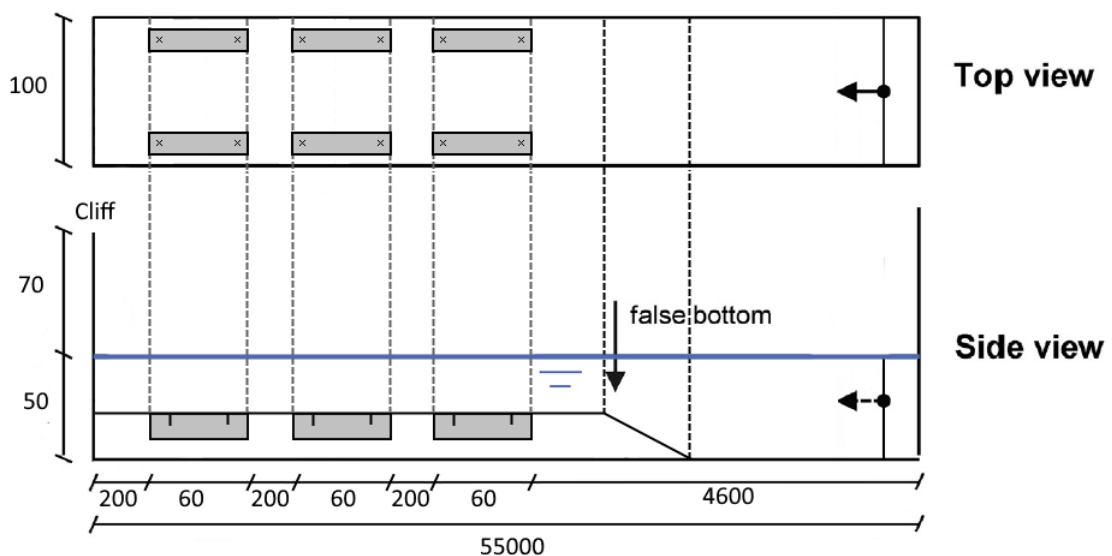


Figure 2.2: A sketch with dimensions of the test set-up in the wave flume (with distances given in cm)

Three types of measurement devices were installed at different locations in the flume. Six Wave Height Meters (WHM), three Flow Velocity Meters (SHM) and three Ultrasonic High Concentration Meters (UHCM) were installed in the flume. The location of these measurement devices in the flume is illustrated in figure 2.3. The wave height meters were distributed over the flume length and placed in the middle of the flume at the still water line ($z=0$). Each flow velocity meter was located in the middle of the flume near the bed between a pair of sample boxes. At these locations, the flow velocity was measured in both the x and y-direction. The Ultrasonic High Concentration Meters were placed right next to the seedlings in the boxes. The output of the meters was documented every 25 ms. These meters can potentially indicate if the seedlings have failed, in case the water is too turbid to observe this failure with

the naked eye. In this research the plants are deemed to have failed when flushed away or flat against the bed.

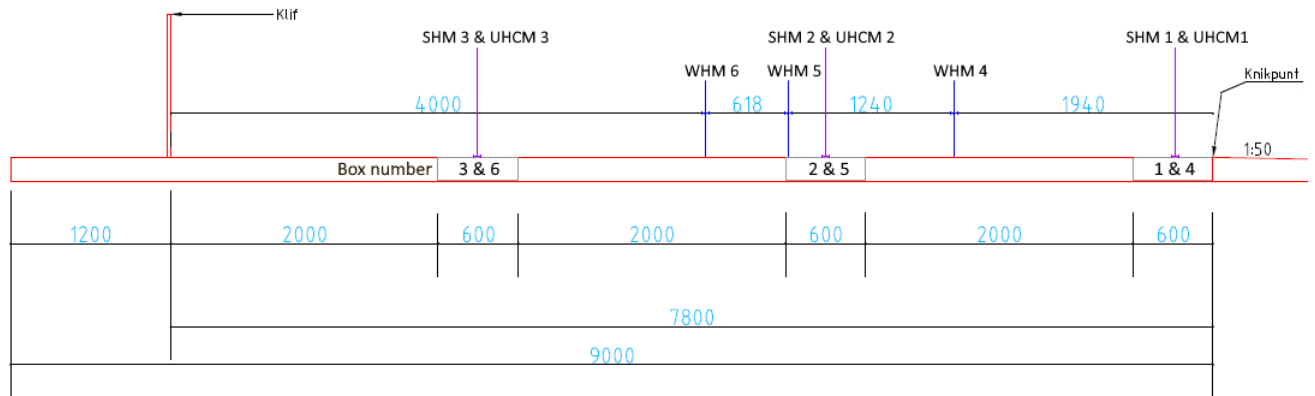


Figure 2.3: Location of the different measurement devices in the flume (with distances given in millimeters)

The flume could accommodate six separate boxes per run. Each test in the flume had a maximum duration of 30 minutes. However, if a plant's failure was observed during the experiment, the run was shut down. The erosion around the collapsed plant was measured using a calliper. This ensured that the erosion depth around the plant at the time of the failure was documented, and prevented the scour-holes from being washed away once the plants had failed.

The total erosion that induced seedling toppling was recorded as the critical erosion depth (CED). After finalising a run, all boxes were examined and the erosion around the plants was measured using a calliper. If the plants in a box appeared not to have failed, another run could be added to examine the effect of more prolonged exposure to wave loading.

After the box was removed from the flume, the belowground plant biomass of the seedlings was measured. Each plant was carefully dug out of the sediment. The root length and root thickness were measured using a ruler and calliper respectively, and the plants were again photographed.

Table 2.2: Overview boxes in the flume and wave characteristics

Sediment	Number of Boxes	Number of Samples	vegetation Species	Wave period (s)	Amplification factor	Waveheight (m)
Sand	12	24	<i>Salicornia procumbens</i>	2.5	0.5-0.8	0.125-0.2
Clay	9	13	<i>Salicornia procumbens</i>	2.5	0.5-0.8	0.125-0.2

2.2 Flume experiment: sediment characteristics of fresh mud

In addition to the failure of *Salicornia* seedlings, the erosion of freshly deposited cohesive sediment under wave loading was also investigated. Section 2.2.1 describes the preparation of the samples before entering the flume. Section 2.2.2 presents the measurement techniques used during the flume experiment.

2.2.1 Flume sample preparation

Ten of the rectangular boxes were filled with homogenised Zuidgors sediment. This was done in two intervals, so samples were available in which the mud had settled for one day and in which the mud had settled for five days. Two boxes of each time interval were not tested in the wave flume, but were used to determine the shear strength. The shear strength (kPa) of these sediments was determined using a shear vane. Each box was sufficiently large so at least two shear measurements could be conducted.

The consolidation of the boxes containing fresh (newly homogenised) mud was measured before being placed in the flume. The consolidation was measured at six locations in the box (at the corners and in the middle at both sides) using a ruler. These six measurements were then used to calculate an overall mean value for the consolidation per box.

In six of the boxes, two rods were placed at approximately the place the seedlings would be located. These rods indicated how scour-holes develop in fresh mud. The boxes were photographed before being placed in the flume.

2.2.2 Flume tests and measurements

The boxes were placed in the flume and received wave loading in periods of 30 min. The waves produced by the flume were irregular with a peak period of 2.5 seconds

and an amplification factor of 0.8, which equates to a significant wave height of 0.2 m. This setup was equal to the setup used while testing the *Salicornia* seedlings. The boxes were placed in the flume for up to 120 minutes or four runs. After every interval, the boxes were removed from the flume to document the development of the sediment. The erosion in the boxes was measured using the same procedure as the measurement of consolidation in the boxes. Finally, the scour-hole depth around the poles was determined using a calliper.

2.3 Calculation of plant traits

Some of the plant traits, like the frontal surface area of the seedlings and the surface area of the root system, were not directly measured but were calculated subsequently. Section 2.3.1 describes the calculation of the frontal surface area of the seedlings. Section 2.3.2 presents the calculation of the root system area. Section 2.3.3 explains the determination of the density of fresh *Salicornia*.

2.3.1 Frontal surface area of the aboveground biomass

During the flume experiment the plants were photographed in front of a white background. The background included a scale (2 cm). The frontal surface area of the plants was subsequently determined using photoshop. In photoshop the frontal surface area of a plant was calculated by comparing the number of pixels of the plant picture with the number of pixels of the scale included in the background. This calculation was done for all samples and the resulting frontal surface area of each plant was documented in square mm.

2.3.2 Surface area of the root system

For the root system a similar approach was taken. The root systems were photographed after concluding the stay in the flume. The samples were again photographed in front of a white background, including a scale and then the area of the root system was determined using photoshop. The roots presented more challenges than the aboveground biomass because some of the roots broke off during the flume experiment and there was still some sediment present in some samples, which had to be accounted for. The root surface area was documented in square mm.

2.3.3 Density of fresh *Salicornia*

Fresh *Salicornia* has a density of 433.33 kg/m^3 . The density was measured by weighing 100 grams of *Salicornia* stems and then determining the volume by placing the measured 100 grams of *Salicornia* into a measuring cup containing 500 ml of water. Once the *Salicornia* is placed in the cup and completely submerged, the water level in the cup will rise by a certain amount. This amount is then the volume of 100 grams of *Salicornia*. This measurement is repeated three times to reduce measurement uncertainty.

2.4 Calculation time and received energy in the flume

The experiment used irregular waves with a period of 2.5 seconds and an amplification factor of 0.6 to 0.8. For every amplification factor the same wave scenario was used, which lasted approximately 30 minutes. The majority of the samples in the flume did not fail after a single run and were therefore subjected to several subsequent runs with varying amplification factors. Comparing the seedling by using the time occupied in the flume may give skewed results, because the wave scenario with an amplification factor of 0.6 will have less wave energy than a wave scenario with an amplification factor of 0.8. Two methods were used to compensate for the varying amplification factors. Section 2.4.1 describes the first method, and the second method is presented in section 2.4.2.

2.4.1 Adjusted time in the flume

In the first method the time in the wave flume was adjusted for the amplification factor. For this parameter, the time under each wave scenario was multiplied with the associated amplification factor, to account for the different wave scenarios. If a plant received wave loading from several different wave scenarios, the adjusted time under each scenario was calculated separately and then aggregated.

2.4.2 Energy received by plant and drag force

The second method to compensate for varying amplification factors was to calculate the wave energy received by each plant. The wave energy received by each seedling was calculated using a Matlab script. In the script the relevant data for the calculation were loaded. These included the measured flow velocities at every amplification factor, the duration each plant received wave loading of the separate wave scenarios with varying amplification factors and the relevant bio-morphological plant

properties (plant height, stem diameter, frontal surface area).

Due to the oscillatory nature of the flow velocities generated by waves, the absolute values of the flow were used to calculate the energy received by the plants. First, the drag forces experienced by the plant in each time interval were calculated. For this calculation it was assumed that the plants were cylinders. The drag force per timestep was calculated using Equation 2.1.

$$F_d(z, t) = \frac{1}{2} C_D \rho_w \emptyset_{stem}(z) |u(z, t)| u(z, t) \quad (2.1)$$

Where:

F_d	the drag force (N)
C_d	the drag coefficient ($-$)
ρ_w	the density of water (kg/m^3)
\emptyset_{stem}	the stem diameter of a <i>Salicornia</i> seedling (m)
u	the flow velocity (m/s)
z	the distance from the bed (m)

At each timestep, the drag coefficient C_d can be determined as a function of the Reynolds number (Equation 2.2).

$$C_d = f(Re) = f\left(\frac{U \emptyset_{stem}}{\nu}\right) \quad (2.2)$$

Where:

Re	the Reynolds number ($-$)
U	the average flow velocity (m/s)
ν	the (kinematic) fluid viscosity (m^2/s)

The flow regime, and therefore the drag coefficient, changes with varying flow speeds. Thus, the drag coefficient was calculated separately for every plant at every time step. In the research of Chen et al. (2018) and Nepf (2012) a comprehensive list of the most appropriate calculation of the drag force for each flow regime was given. The complete list of all drag coefficient equations for each flow regime used in this research, can be found in Appendix A. Once the drag force on the plants was known at every timestep, the wave energy at every timestep could be calculated using equation 2.3. This equation integrates the drag force over the plant height. Because plants with a larger frontal surface area receive more energy, a corrected plant height is used that compensates for the larger frontal surface area.

$$\varepsilon_v = \overline{F_d u(z, t)} = \overline{\int_{z=0}^{z=h_v} F_D u(z, t) dz} \text{ with } F_d = \frac{1}{2} \rho_w C_D \emptyset_{stem}(z) N_v |u(z, t)| u(z, t) \quad (2.3)$$

Where:

ε_v	the wave energy dissipation (j)
h_v	the height of the vegetation (m)
N_v	the stem density ($-$)

Finally all timesteps can be combined to determine the total amount of energy a plant has received during the time in the wave flume.

2.5 Forces on the seedlings

Under wave loading several forces are acting on the seedlings. To understand the mechanisms causing failure in seedlings, it is important to identify these forces. Section 2.5.1 explains the buoyancy and gravity forces applied to the aboveground biomass of the seedlings. Section 2.5.2 describes the root anchorage of the seedlings to resist the uprooting forces. Section 2.5.3 describes the momentum forces on the seedlings. The drag force calculation was elaborated in section 2.4.2 when determining the received energy of a seedling, using equations 2.1 and 2.2.

The gravity force (downward force due to the mass of the seedlings) and the buoyancy force, can be calculated using the plant characteristics like the stem diameter, plant height and the density of fresh *Salicornia*.

2.5.1 Calculation of the gravity force and the buoyancy in force balance

For this calculation it is assumed that the forces on the aboveground biomass work on the middle of the plant height (Figure 2.4). Another assumption is that the measured stem diameter is equal over the whole plant stem and that these stems are perfect cylinders.

For the gravity component the weight of the seedling needs to be calculated, using, the plant density. To compensate for any bifurcation and plant complexity, the frontal surface area of each plant is divided by the respective stem diameter (Equation 2.6) resulting in the adjusted plant

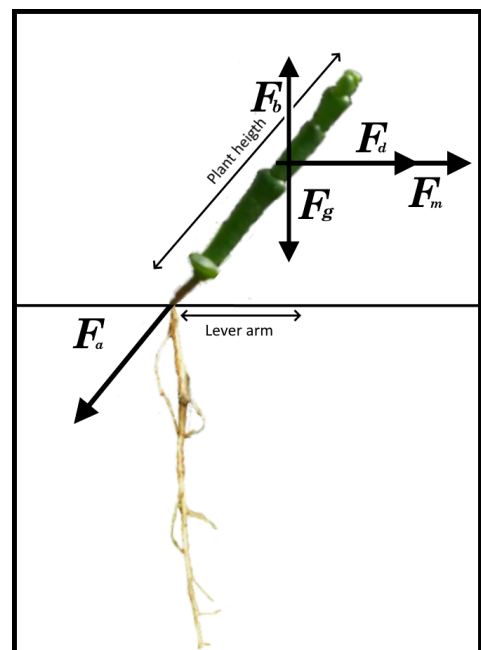


Figure 2.4: Forces on seedling

height. The adjusted plant height is used for the plant mass calculation. The gravity component is then calculated using equation 2.4; the components of this equation are expanded in equations 2.5 and equation 2.6. The result of combining these equations is equation 2.7.

$$F_g = m_{plant} * g \quad (2.4)$$

$$m_{plant} = \rho_{Salicornia} * \frac{1}{4} \pi * \emptyset_{stem}^2 * h_{adjust} \quad (2.5)$$

$$h_{adjust} = \frac{A_{frontal}}{\emptyset_{stem}} \quad (2.6)$$

$$F_g = (\rho_{Salicornia} * \frac{1}{4} \pi * \emptyset_{stem}^2 * h_{adjust}) * g \quad (2.7)$$

Where:

F_g	the gravity force (N)
m_{plant}	the mass of a single seedling (kg)
A	the frontal surface area of a <i>Salicornia</i> seedling (m^2)
$\rho_{Salicornia}$	the density of fresh <i>Salicornia</i> (kg/m^3)
g	the gravitational constant (m^2/s)
h_{adjust}	the plant height adjusted for plant complexity (m)

The buoyancy force is the upward force on the plants when submerged. This force acts in the opposite direction of the downward force by gravity. The buoyancy force has a magnitude directly proportional to the volume of the displaced liquid (equation 2.8).

$$F_b = \rho_w * V_{plant} * g = \rho_w * (\frac{1}{4} \pi * \emptyset_{stem}^2 * h_{adjust}) * g \quad (2.8)$$

Where:

F_b	the buoyancy force (N)
V_{plant}	the volume of a single seedling (m^3)

2.5.2 Root anchorage

The anchorage strength of the seedlings depends on the cohesive strength of the sediment and the size of the root system. In the research of Schutten et al. (2005), several models were presented to determine the root anchorage of certain plant species. These models (equations 2.9 and 2.10) approximated the anchorage strength using the product of cohesive strength and root-system size (Schutten et al., 2005).

In these equations F_a is the anchorage strength (in Newton) and k and j are species-specific attachment coefficients for the surface of a hemispherical root ball.

$$F_a = k * A_r^{\frac{2}{3}} * C_u \quad (2.9)$$

$$F_a = j * M_r^{\frac{2}{3}} * C_u \quad (2.10)$$

Where:

F_a	the anchorage force (N)
A_r	the root area (m^2)
M_r	the root dry mass (g)
C_u	the sediment cohesion (Pa)

The research of Schutten et al. (2005) showed that these models were able to predict anchorage strength reasonably well for all of the nine species investigated. *Salicornia procumbens* was, not one of the species that was tested. During the flume experiment, the dry mass of the root systems of the samples was not measured. However, the bio-morphology of the root system and the cohesion were determined. So in this research, the model for the anchorage described by equation 2.9 is used. To use this model, the species-specific attachment coefficients for the surface of a hemispherical root ball need to be determined. This parameter can be determined by rewriting equation 2.9 and using the removal force of *Salicornia* that was measured from several samples during the experiment.

$$k = \frac{F_a}{A_r^{\frac{2}{3}} * C_u} \quad (2.11)$$

This dimensionless parameter can be determined with the measured shear strength and bio-morphology of the root system (equation 2.11). This calculation was conducted using all samples in which the removal force was measured. The average will be used as the specific attachment coefficient for *Salicornia* (Appendix C). This parameter could then be used to determine the anchorage strength of the samples in which the removal force or anchorage was not directly measured.

2.5.3 Dynamic force on seedling, momentum

Due to the oscillatory nature of flows produced by waves, the flow direction periodically reverses and the plant is swept in the flow direction. This constant acceleration and deceleration of the aboveground biomass of the plant, gives a certain momentum. The force produced by the constantly changing momentum adds to the forces

pulling on the root system. For the calculation of the force exerted by the momentum, it is assumed that the movement speed of the plant is equal to the orbital speed of the flows produced by the waves. Furthermore, it is assumed that this speed is reached instantly and starts at 0 when the plant is completely swept to one side. The force produced can be calculated using equation 2.12 .

$$F_m = \frac{dp}{dt} = m * \frac{dv}{dt} \quad (2.12)$$

Where:

F_m	the momentum force (N)
d_p/d_t	the rate of momentum transfer per unit time ($kg * m/s$)
d_v/d_t	the change in velocity per unit time (m/s)

The mass of the plants can be derived from the plant traits using the same procedure as calculating the gravity force (Equation 2.5).

For smaller plants, the force produced by a change in momentum is often minor compared to the drag forces. The factors that scale with mass like the momentum forces on the plants are likely to increase more rapidly with increases in size than are factors that scale with the area such as the drag forces. So in small, lightweight plants, the drag forces may be dominant, whereas, in large plants, the force due to momentum is dominant. In the research of Denny et al. (1998), a dimensionless index, the jerk number (Equation 2.13), is proposed as a tool for predicting when inertial forces will be important. This jerk number will be used to assess if the momentum force is a dominant force acting on the *Salicornia* seedlings in this research. This number is the maximal inertial force that could be applied to the plant divided by the maximal drag force Denny1998TheOrganisms. For this calculation, it is assumed that the maximum flow velocity during the experiment was 0.60 m/s.

$$J = \frac{u_{x,m} \sqrt{km}}{F_{D,max}} \quad (2.13)$$

2.6 Bed shear stress

In this section the determination of the bed shear stress, using the flow velocities is described. Bed shear stress is a fundamental parameter, that links flow conditions produced by waves to sediment transport and erosion. The bed shear stress (τ_b) can be calculated using equation 2.14 from Van Rijn et al. (1993) and the equivalent bed roughness (equation 2.15) f_w using the equation provided by Soulsby (1997).

$$\tau_b = \rho_w u_*^2 = \frac{1}{2} \rho_w f_w U_b^2 \quad (2.14)$$

$$f_w = 1.39 \left(\frac{A_w}{z_0} \right)^{-0.52} \quad (2.15)$$

$$z_0 = \frac{K_N}{30} = \frac{D50}{12} \quad (2.16)$$

$$K_N = 2.5 * D50 \quad (2.17)$$

Where:

τ_b	the bed shear stress (Pa)
f_w	the wave friction coefficient (–)
U_b	the near bed flow velocity (m/s)
z_0	the roughness length (m)
K_N	the Nikuradse roughness height (m)
A_w	the wave orbital semi-excursion at the bottom (m)
$D50$	the maximum median sediment diameter (mm)

To determine if the flow velocities produced by the wave flume result in sediment transport, the critical shear stress of the sediment is compared to the shear stresses produced by the flow velocities. The critical shear stress of the sand used during the flume experiment, was approximately 0.14 Pa (Schroevers et al., 2010; You et al., 2009) (Figure 2.5). In the same table, the value for consolidated sand with 50% clay ranges from 0.50 to 1.00 Pa. The Zuidgors sediment had a 60.5% silt fraction and was very consolidated, so the critical shear stress was estimated to be in the upper limit of this range (1.00 Pa).

Sediment type	Critical shear stress (τ_{crit} [N/m ²])	
	<i>Incipient motion</i>	<i>Transport of suspended material</i>
Sand (D50 = 100 μ m)	0.14	0.2
Sand (D50 = 250 μ m)	0.19	0.5
Sand (D50 = 400 μ m)	0.23	0.7
Sand with 50% slit (nonconsolidated)	0.3 – 0.8	-
Sand with 50% slit (consolidated)	0.5 – 1.0	-

Figure 2.5: Critical shear stress (τ_{crit}) for different types of sediment (Schroevens et al., 2010)

2.7 Statistical methods

Section 2.7.1 presents the method for determining the average and standard deviation of the plant traits per age group. Section 2.7.2 describes the Student's T-test used to determine if certain parameters like scour depth in sand or clay were statistically different.

2.7.1 Averages and standard deviation

To calculate the averages and standard deviations of the observed plant traits, seedlings of ascending ages were distributed over bins of 5 days. The average and standard deviation within each bin was calculated. The averages and standard deviation over time were plotted in Matlab to compare the results and give a comprehensible view. The standard deviation was used for the error bands of the averages at each time interval.

2.7.2 Significance of the difference (T-test)

The T-test is a parametric statistic test. It is generally used to examine if the population mean differs from a certain value using a null hypothesis (Mcclave et al., 2011). It was assumed that the variance of the different populations was not equal and the test was two-sided. The confidence interval used was 0.05, which is a typical confidence interval in science (Mcclave et al., 2011). The default null hypothesis for a 2-sample t-test is that the two groups are equal. So, the null hypothesis is rejected when $P < 0.05$. Rejection of the null hypothesis indicates that the compared parame-

ters are statistically different at the chosen confidence interval. Using equation 2.18, the T-value is then calculated.

$$t = \frac{\bar{x}_i - \bar{x}_j}{\sigma\sqrt{n}} \quad (2.18)$$

Where:

t	the T-test value (–)
\bar{x}_i	the sample mean (–)
\bar{x}_j	the population mean (–)
σ	the standard deviation (–)
n	the population size (–)

Results

This chapter presents the results of the research. The chapter starts with the development of the sediments over time presented in section 3.1. This section is followed by section 3.2, presenting the development of the *Salicornia* seedlings in these different sediments. Next, in sections 3.3 to 3.6, the failure of the seedlings in the wave flume is presented. Last, section 3.7 the additions to the WoO framework as a result of the findings of the research are described.

3.1 Development of sediment over time

The shear strength of cohesive sediments measured during the flume experiment is higher and more variable than the shear strength of non-cohesive sediments (Table 3.1), although it should be taken into account that this included the tests with fresh mud that had only settled for five days. Excluding these samples, the range of the shear strength is still more variable in cohesive sediment and overall higher. The cohesive sediment exhibited considerable consolidation over time (Figure 3.1). The consolidation rate flattened out over time; therefore, consolidation in cohesive sediments is not linear. The sandy sediment on the other hand, exhibited no consolidation.

The erosion resistance of the cohesive sediment rapidly increased over time. Figure 3.2 shows how older mud behaves in comparison to freshly deposited mud.

Table 3.1: shear strengths ranges of the different sediment types

Sediment type	Observed shear strength range
Non-cohesive	7.20-28.85 kPa
Cohesive	15.30-68.40 kPa
Cohesive (including five-day-old samples)	0.50-68.40 kPa

Fresh, one-day-old sediment erodes easily under the wave conditions produced in the flume with erosion rates between 0.17 and 0.5 mm per minute. This erosion process seems to have a linear characterisation. For mud that has settled for five days, the erosion rates in the flume are lower, between 0.14 and 0.11 mm per minute. However, this process was not linear. Once the top layer of the sediment had eroded, the erosion rate seemed to reach an equilibrium in which longer commensurate wave loading did not result in more erosion (Figure 3.2).

The cohesive sediment in which the *Salicornia* seedlings were planted was much older (70+ days) than the 5-day old samples and therefore experienced considerable consolidation. The erosion resistance of this sediment was so high that even at maximum amplification in the wave flume, hardly any erosion occurred in these samples

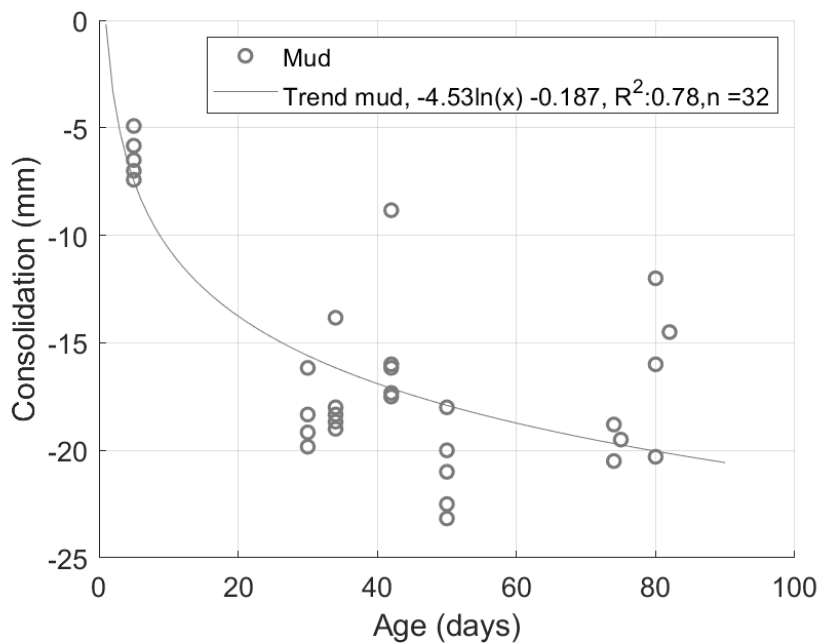


Figure 3.1: Consolidation cohesive sediment over time

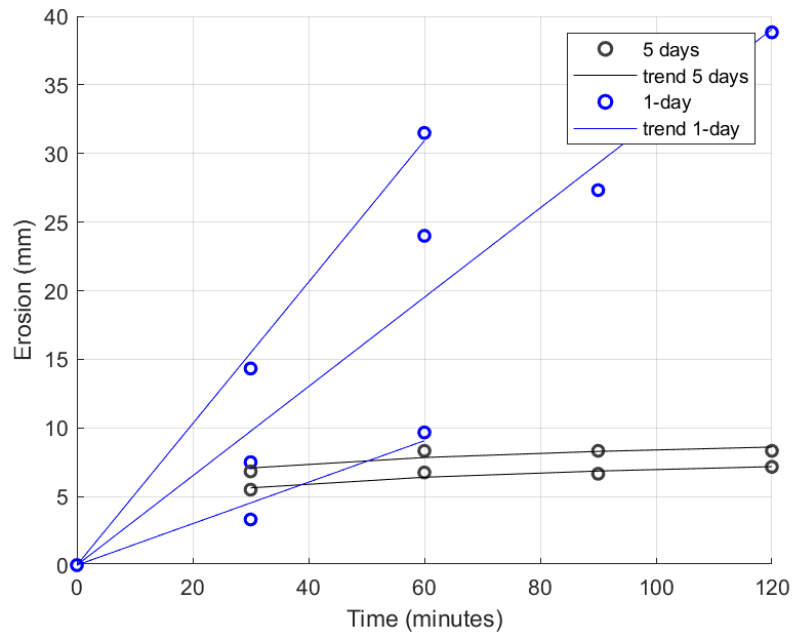


Figure 3.2: Erosion in flume over time for cohesive sediment, one day old (blue) mud, five days old mud (black)

3.2 Development *Salicornia* seedlings in different sediments

The development of the *Salicornia* seedlings is divided into the development of the aboveground biomass and the belowground biomass. Section 3.2.1 describes the development of the seedlings aboveground. Section 3.2.2 describes the development of the seedlings belowground.

The aboveground biomass consists of the length of the shoot, diameter of the stem and the total frontal surface area of the plant. The belowground biomass is the length of the roots and the thickness of the roots.

3.2.1 Morphological plant characteristics of the aboveground biomass

The development of plant height over time is comparable for seedlings growing in sand and mud (Figure 3.3). Although the linear fit for mud seems to be slightly steeper and higher, the plant height is not statistically different in seedlings growing in sand and mud ($P= 0.735$). Furthermore, the plant height of the seedlings growing

in mud seems more variable than those in sand, with a larger standard deviation per age group (Figure 3.6). This trend continues for the frontal area and stem diameter; especially, the average frontal surface area of seedlings in mud is larger with an even larger standard deviation (Figure 3.7 and Figure 3.8). However, both the frontal surface area and stem diameter are not statistically different ($P=0.056$) and ($P=0.178$).

Figure 3.4 suggests that in muddy sediments, the seedlings develop a larger frontal surface area in the same period compared to sand. In figure 3.7, this is visible. Overall, the frontal surface area of the seedlings in mud is larger at a specific plant height than in sand (Figure 3.5). This suggests that the aboveground biomass of the plants in mud becomes more complex in a shorter period. Figure 3.5 also indicates that once a certain plant height is reached, the frontal surface area's development increases more rapidly; this is not a linear process.

In terms of observed plant morphology of the aboveground biomass, there are some differences between seedlings growing in sand and mud. In mud, the main stem sprouts a few primary branches that often bifurcates into secondary branches. With increasing plant height, the plant becomes more complex with more branches and secondary branches. In sand, the emerging seedlings consist of a thin main stem, sometimes with a few short primary branches, but overall the plants are less complex than their counterparts in mud.

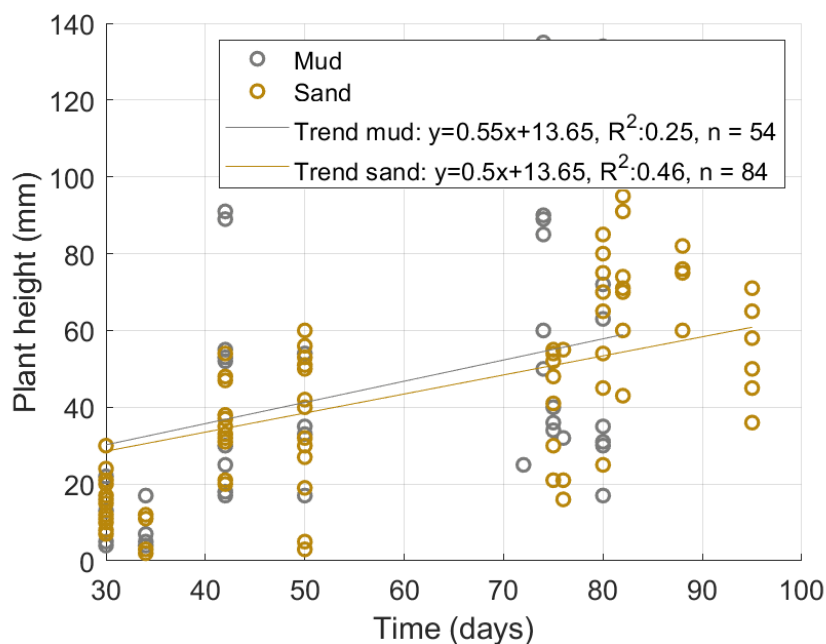


Figure 3.3: Plant height (mm) vs age (days)

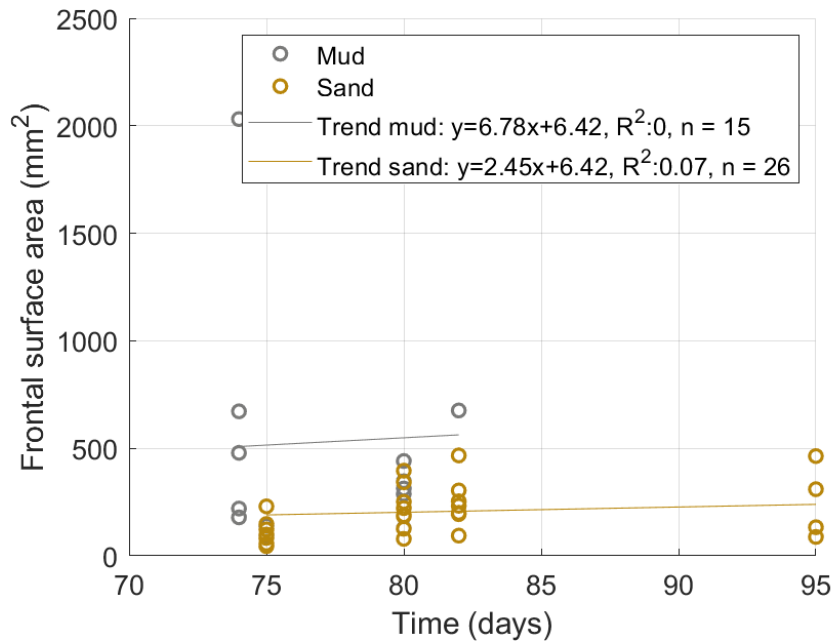


Figure 3.4: Frontal surface area (mm^2) vs age (days)

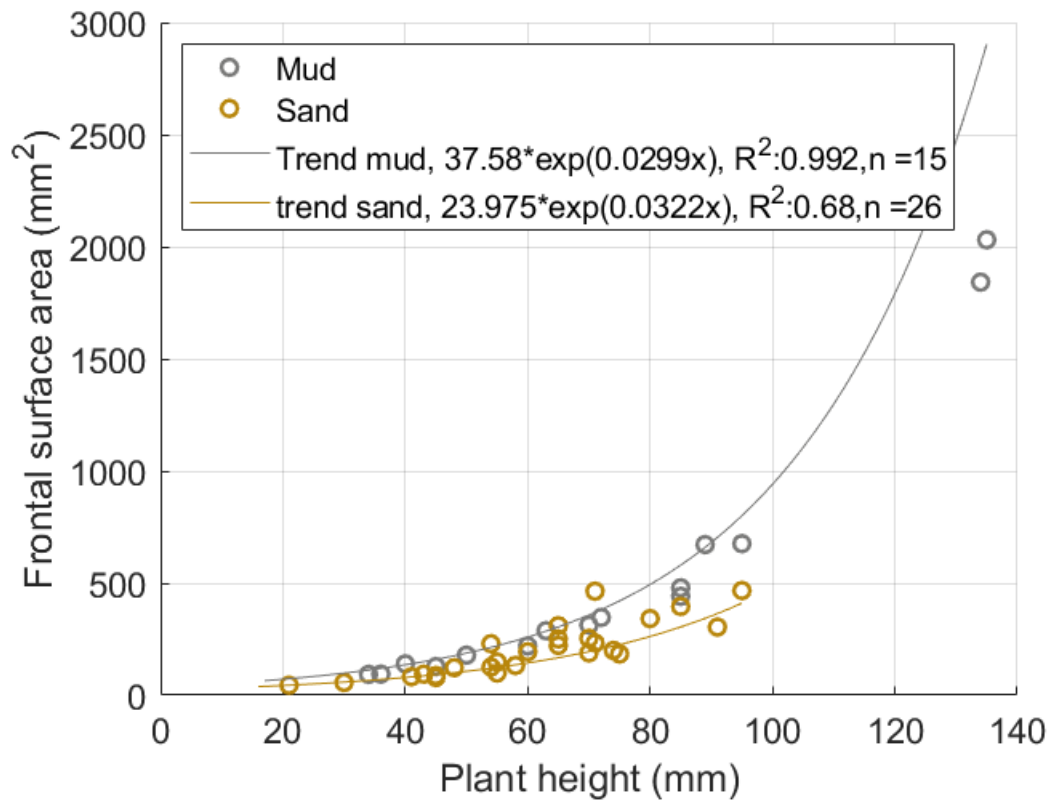


Figure 3.5: Plant height (mm) vs frontal surface area (mm^2)

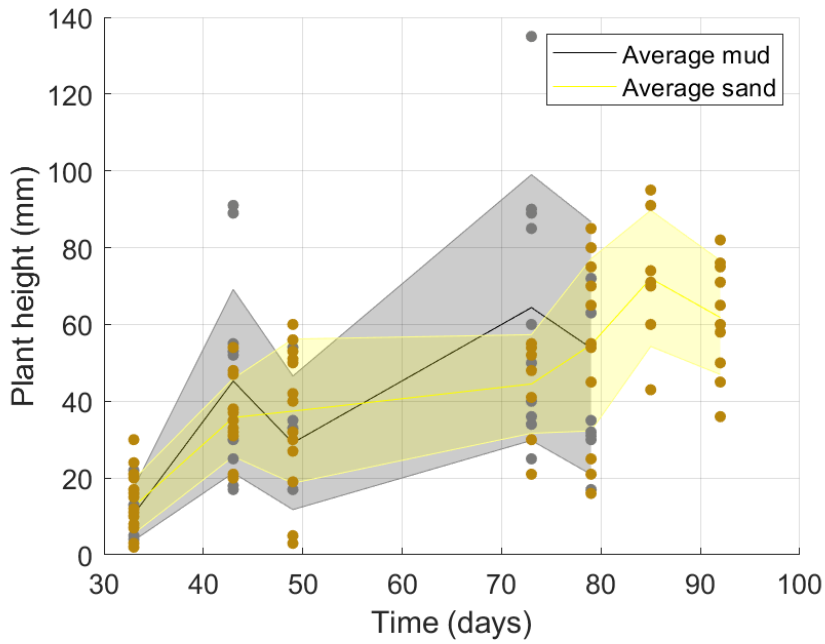


Figure 3.6: Plant height (mm) vs age (days) average with standard deviation

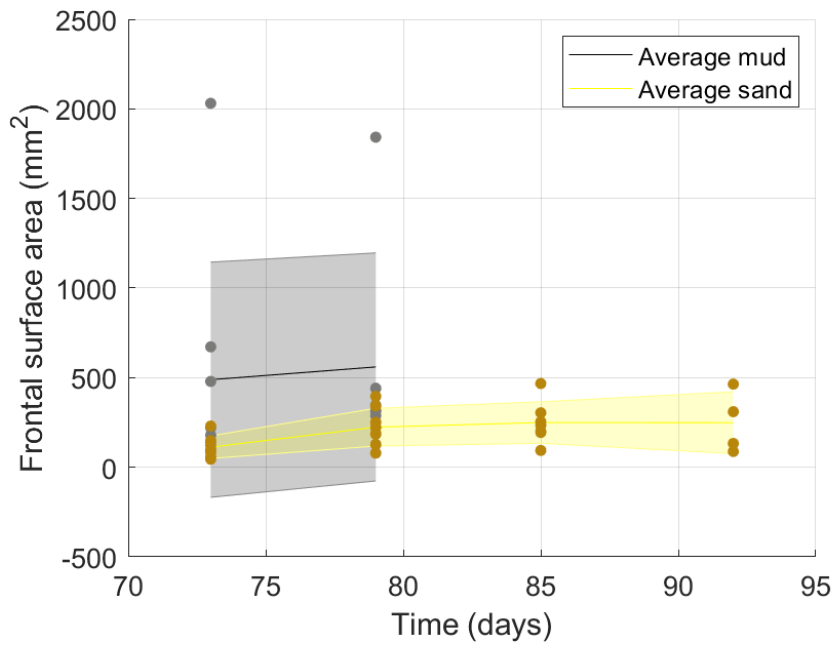


Figure 3.7: Frontal surface area (mm^2) vs age (days) average with standard deviation

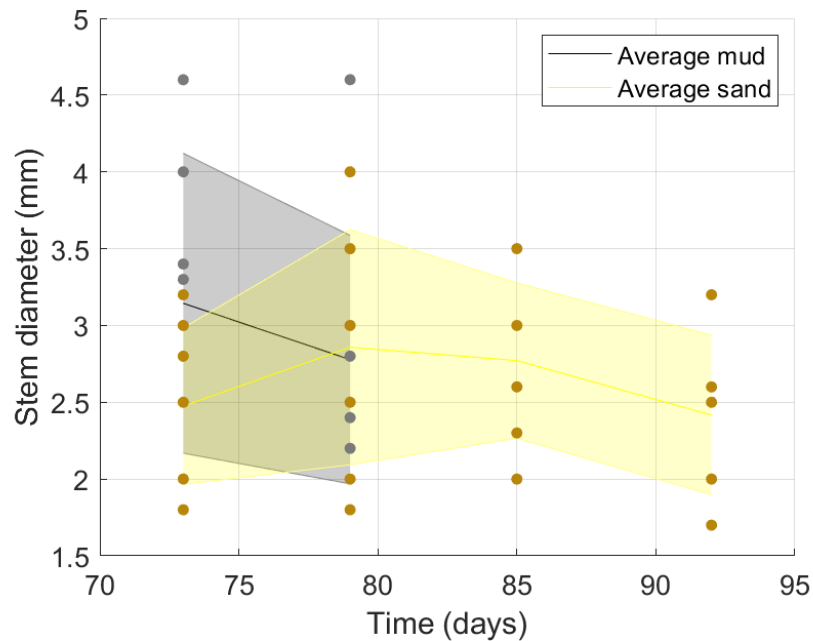


Figure 3.8: Stem diameter (mm) vs age (days) average with standard deviation

3.2.2 Morphological plant characteristics of the belowground biomass

In terms of observed plant morphology of the belowground biomass, there are some differences between seedlings growing in sand and mud. The root length and root thickness are statistically different between sand and mud ($P=0.027$) and ($P=0.003$). Figure 3.9 shows that roots growing in sand are, on average, thinner and longer compared to roots growing in mud. These differences are also visible in figures 3.10 and 3.11, comparing the averages and standard deviations of different age groups in sand and mud. Figure 3.11 also indicates a lower variability in root thickness in sand compared to mud.

In sand, a wide and complex root system develops with many bifurcations and a lot of surface area (observation during the experiment). In (consolidated) mud, the *Salicornia* seedlings develop thick and relatively short roots. The root system in mud is simple and narrow, with a thick primary root and a few primary branches to the side (observation during the experiment).

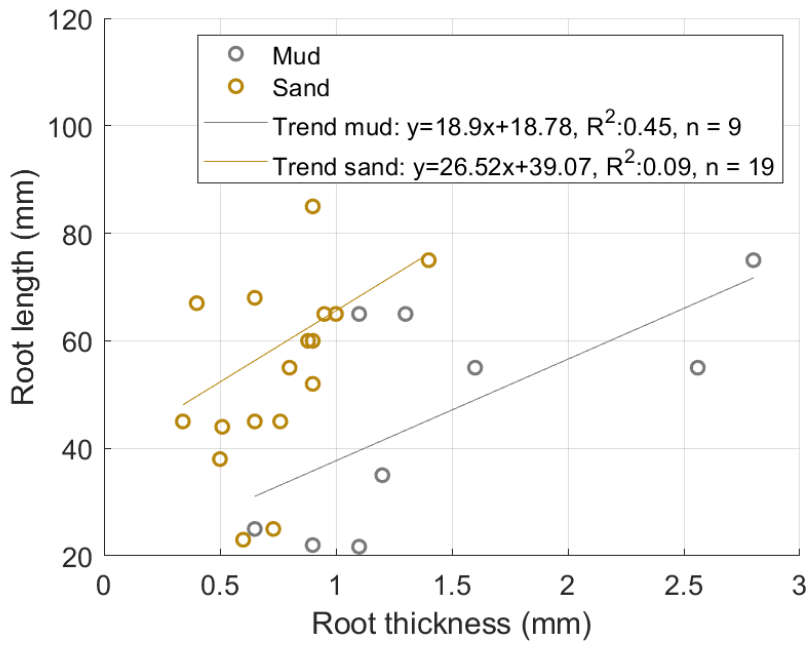


Figure 3.9: Root length of *Salicornia* compared to root thickness in mud and sand

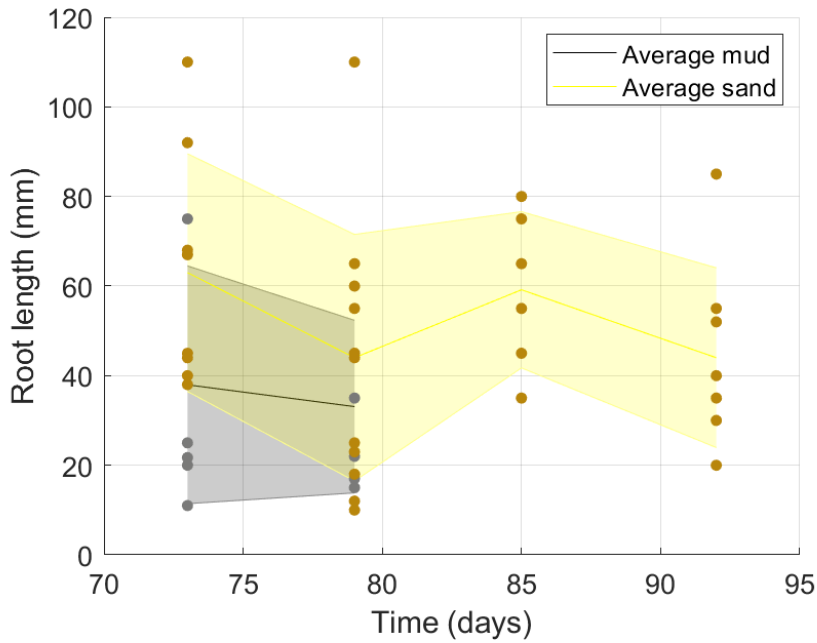


Figure 3.10: Root length (mm) vs age (days) average with standard deviation

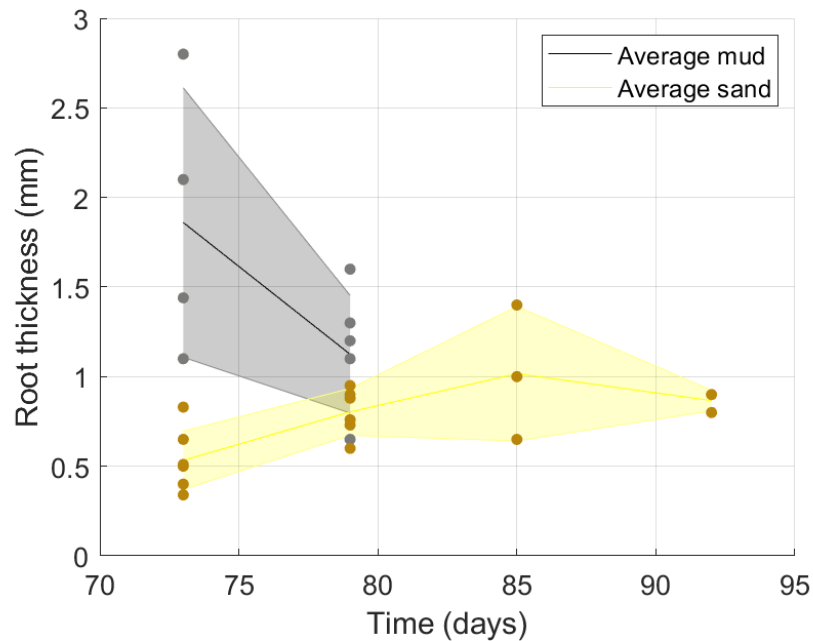


Figure 3.11: Root thickness (mm) vs age (days) average with standard deviation

3.3 Effect of plant traits on failure

In this paragraph the effect of the plant traits on the failure of *Salicornia* seedlings is discussed. The difference in failure because of sediment type is examined in paragraph 3.4. For this analysis, the time in flume adjusted to the wave amplification factor is used.

Figure 3.12 indicates that the aboveground and belowground plant characteristics in mud have a weak correlation with an R^2 value of 0.49. Therefore changes in aboveground biomass may also be the result of changes in the belowground biomass. In sand, the R^2 value is 0.09, this is very low, so in sand the shoot length and root length are independent .

The morphology of the roots seems to influence the failure of *Salicornia* seedlings. The root length has a pronounced positive effect on the amount of wave loading a seedling can endure in both sediments. This trend is presented in figure 3.13D. The effect of the root thickness is less conclusive however (Figure 3.13E). It seems that in non-cohesive sediment the root thickness has no effect on failure.

The effect of the aboveground biomass on the failure of *Salicornia* also seems less conclusive. The different sediments give different results. This difference could result from the correlation between the root and shoot of plants growing in cohesive

sediment. When looking only at non-cohesive sediments, a larger plant height or diameter results in less time in the flume, i.e quicker failure (Figure 3.13A and Figure 3.13B). For all plant trait of the seedlings growing in cohesive sediment it should be noted that the number of samples is limited.

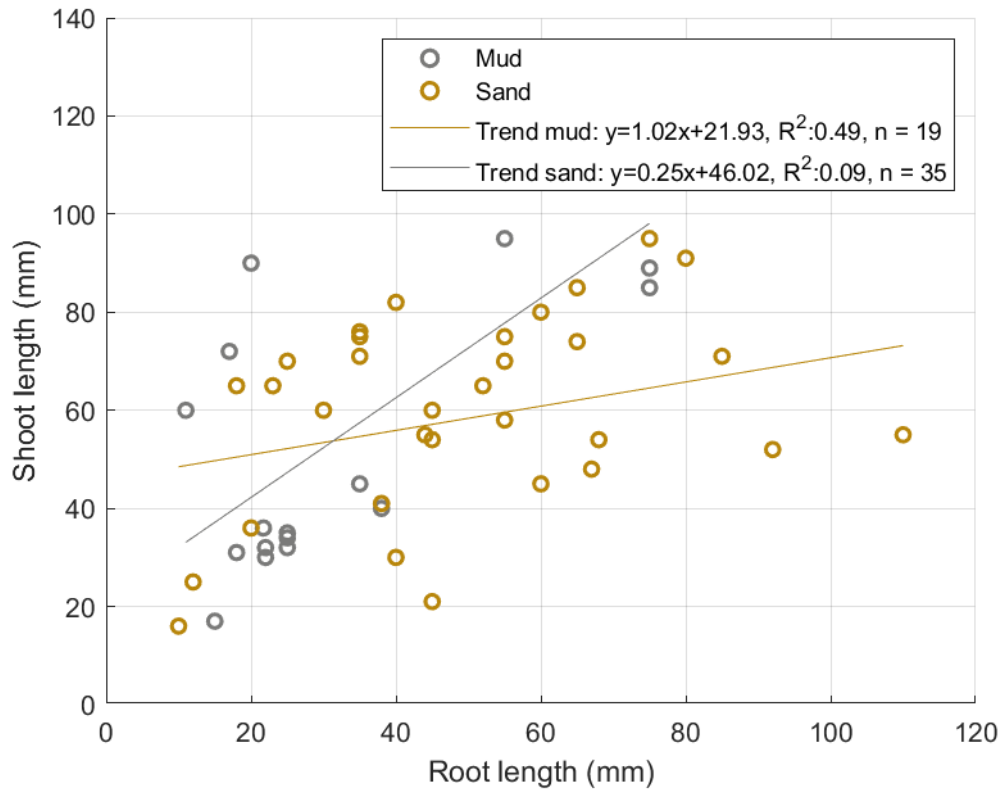


Figure 3.12: Shoot length compared to root length of *Salicornia* in sand and mud

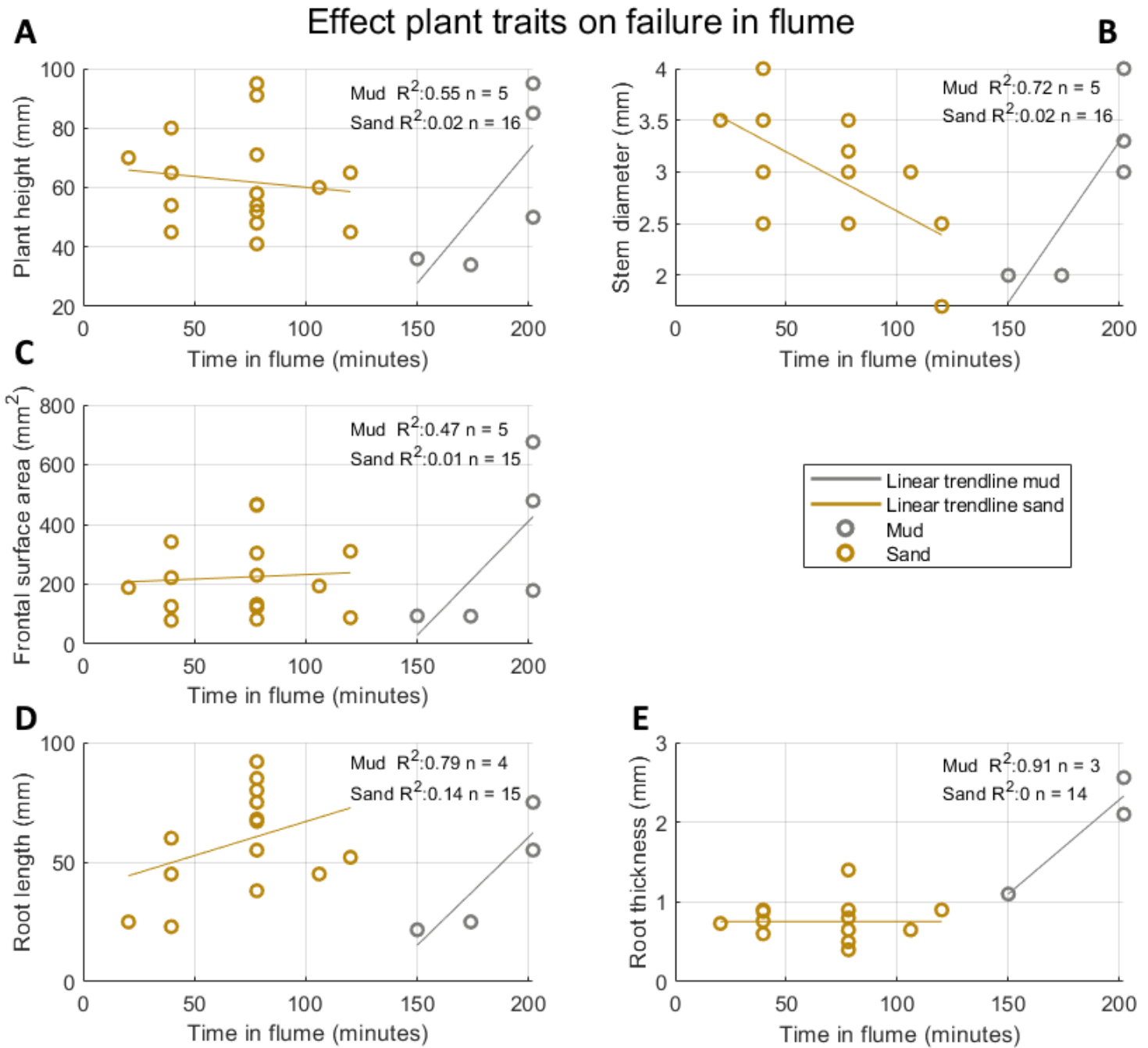


Figure 3.13: Effect of plant traits on the time to failure of *Salicornia* in the wave flume. A: the effect of the plant height; B: the effect of the stem diameter; C: the effect of the frontal surface area; D: the effect of the root length; E: the effect of the root thickness.

3.4 Seedlings under irregular waves

Figure 3.14A shows the flow velocity produced by irregular waves of a wave spectrum with an amplification factor of 0.8 ($H_s=0.20$ m; $T=2.50$ s). The figure shows the velocities produced by the irregular waves during a time interval of 100 seconds; the whole wave spectrum has a duration of approximately 30 minutes. The waves exhibited periods of high flow velocity (for example, at the interval 40-50 s) and periods in which the flow velocity was moderate (for example, at the interval 60-70 s). Over the entire spectrum, the waves produced maximum peak velocities reaching up to 0.82 m/s. These calm and more intense periods are even more pronounced when looking at the bed shear stresses produced by these waves (Figure 3.14B). The reason for this is because the bed shear stress is proportional to the square of the velocity (Equation 2.14). The bed shear stresses produced by the waves over the entire spectrum reached a maximum of 2.05 Pa with an average value of 0.58 Pa.

The non-cohesive sandy sediment had a critical bed shear stress of 0.14 Pa, so the irregular waves should easily be able to cause sediment transport in these samples. This was also observed in the flume, where different erosion and sediment transport patterns were visible. The cohesive Zuidgors sediment had a theoretical, critical bed shear stress of 1.00 Pa. So the irregular waves were occasionally able to erode the sediments during periods with high flow velocity peaks. For example, between 40 and 50 seconds, the bed shear stress exceeds the critical bed shear stress of the sediment and thus, sediment transport may occur. However, for the most part, the bed shear stress produced by these waves remains below the critical bed shear stress, so sediment transport is limited. This was again visible in the flume; the cohesive sediment sample only exhibited minor erosion and little sediment transport.

The energy received by the plants is not only depending on the wave characteristics but also on the aboveground plant parameters. During the experiment, the differences in plant growth between the sediment types were noted. A typical plant in mud (plant 15a) and a typical plant in sand (plant 34a) were selected to examine

Table 3.2: Aboveground plant characteristics of a typical plant in mud and a typical plant in sand

Plant	Height (mm)	Stem diameter (mm)	Area (mm ²)
Typical plant in mud (15a)	70	3.00	313
Typical plant in sand (34a)	54	3.20	230

the effect of the different sediment types. Table 3.2 shows the aboveground plant parameters of these plants used for the wave energy calculation (Chapter 2.4.2). The resulting cumulative energy received by the plants over time during an equal wave scenario (amplification factor 0.8) of 30 min in the flume is presented in figure 3.15. A typical plant in mud has more complexity and, therefore, frontal surface area. Thus, a typical plant in mud receives more energy over time compared to its counterpart in sand; this is visible in figure 3.15. For plant failure, this also means that the root system of plants in cohesive sediment needs to counter higher drag forces compared to plants in non-cohesive sediment.

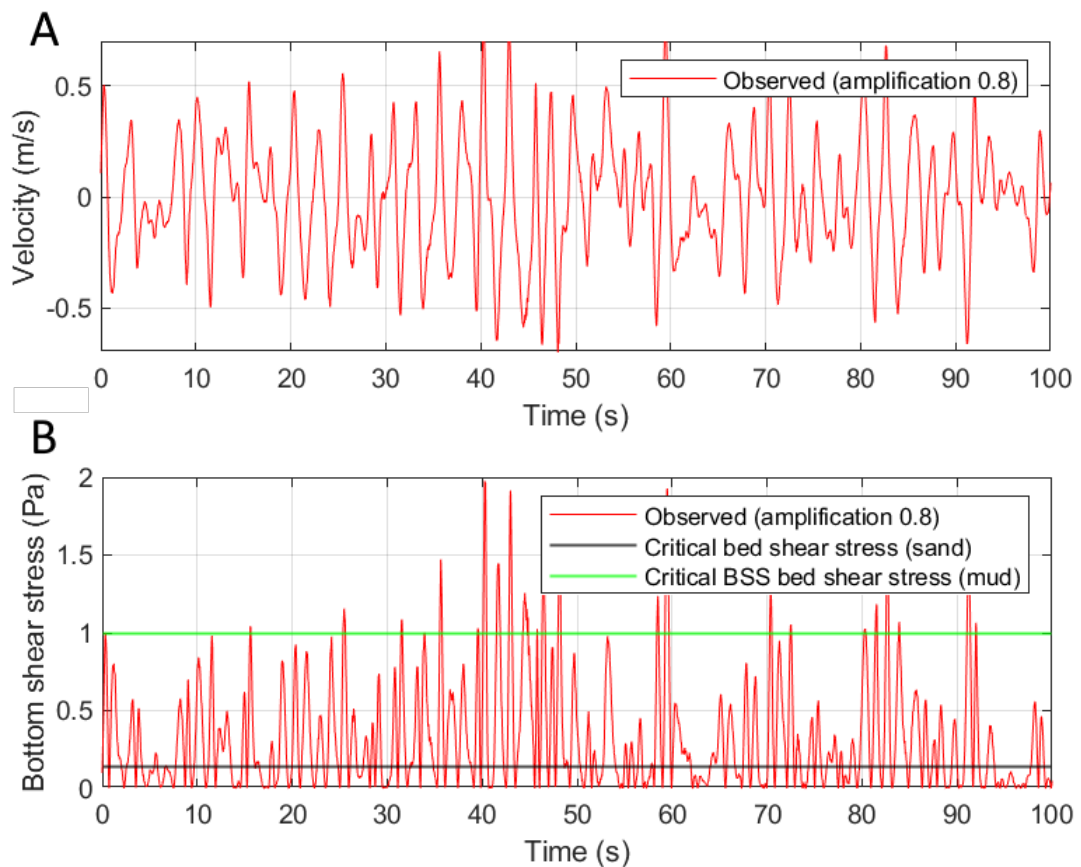


Figure 3.14: A: flow velocities produced by an irregular wave spectrum (top), B: Bed shear stresses produced by an irregular wave spectrum (bottom)

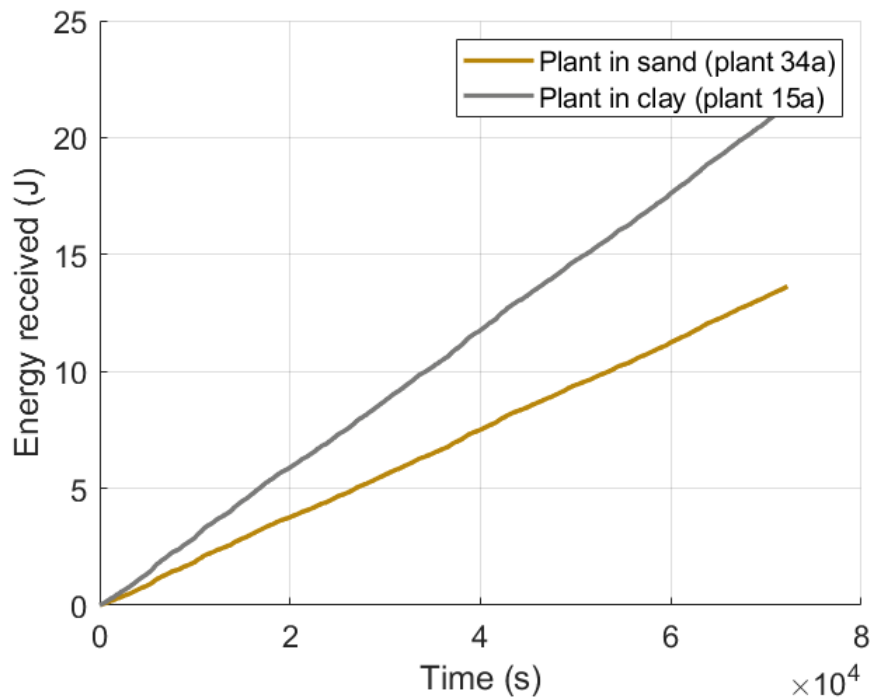


Figure 3.15: Wave energy received by plants under irregular waves in different sediments

The to-and-fro motion as a result of the oscillating flows produced by the waves was not uniform over time, due to the irregularity of the wave spectrum. The movement of the plants varied, between short motions and motions with a longer path that occurred randomly. Figure 3.16 presents the maximum plant movement at two separate time intervals under the same wave scenario. At the lower flow velocity peaks, visible in figure 3.14A, plant motion will be moderate and the extension of the plant stem limited (Figure 3.16A). The plant motion is more intense at the larger peaks however, and will therefore put more strain on the root system (Figure 3.16B); in particular, the lateral roots that have to counter the horizontal movement of the plant are stressed. This stronger force on the lateral roots is illustrated in figure 3.17.

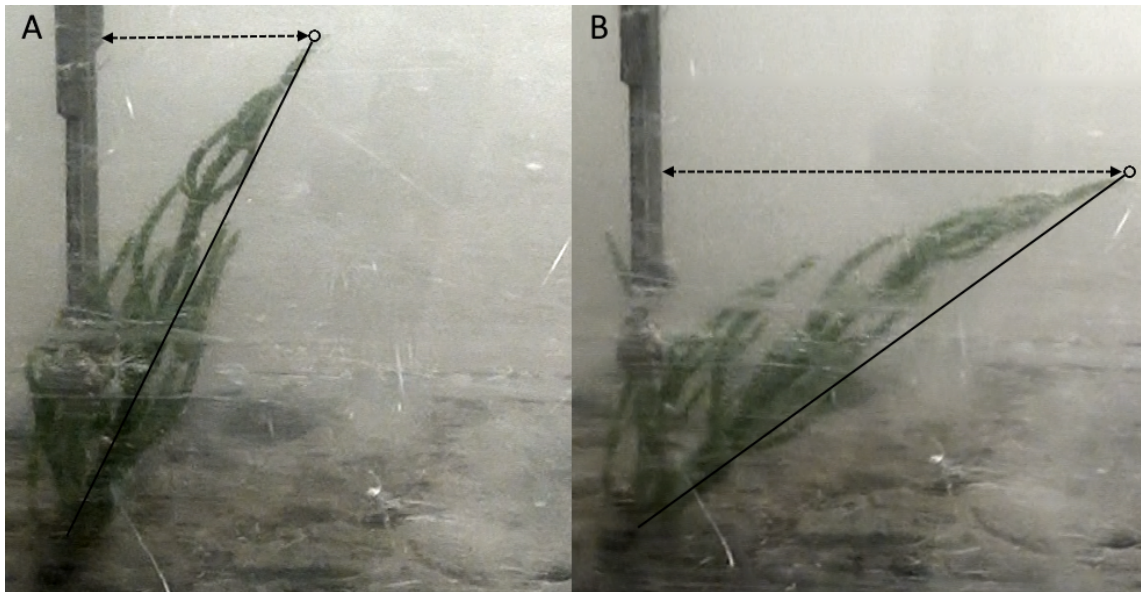


Figure 3.16: Motion path of a seedling under irregular waves, A: moderate flow velocity cause a small motion (left), B: high flow velocities cause a larger motion (right)

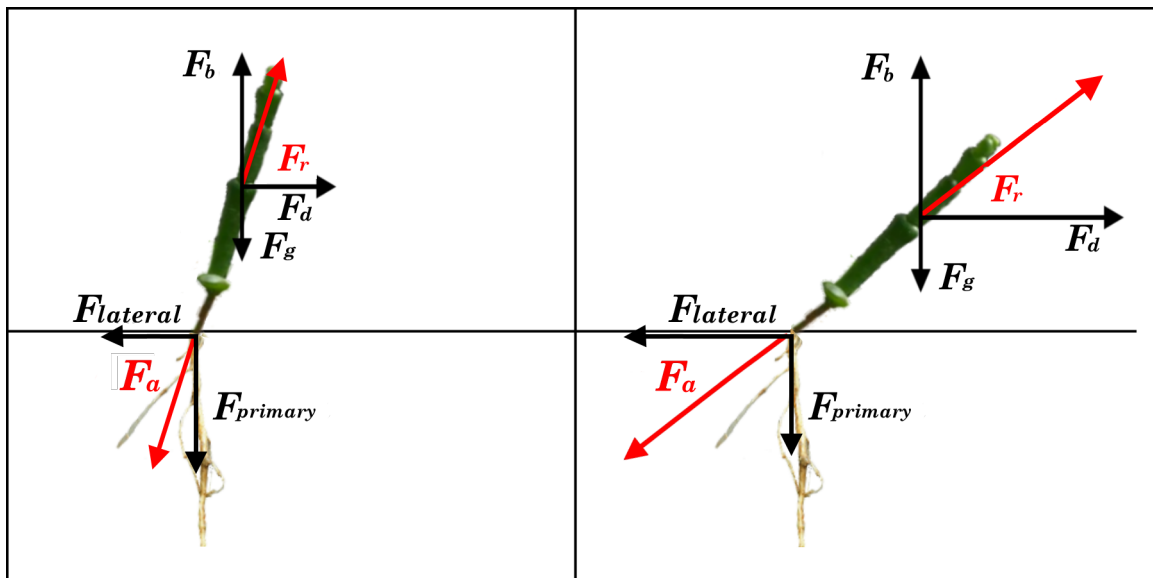


Figure 3.17: Force balance of a seedling under irregular waves, A: moderate flow velocity causes small forces on the root (left), B: high flow velocity causes larger forces on the root (right)

3.5 The different failure mechanisms observed during the flume experiment

During the experiment, the wave-induced failure mechanism exhibited in the flume by the seedlings was different between the sediments. Both scouring and deformation of the sediment around the plants were observed. The different types of depression formation around plants are illustrated in figure 3.18.

In non-cohesive sediment, the wave-induced scouring gradually forms a bowl-shaped depression around the seedlings. The effect of the development of this bowl is to gradually expose the plant roots to the flow and wave action. This reduces root anchoring and unbalances the equilibrium and the seedlings will therefore fail.

In cohesive sediment, the depression around the plant is narrow and uneven; the effect of erosion is less pronounced. During the flume experiment, it was observed that the to-and-fro movement of the plant created these deformation-cavities around the plants. Although still some erosion was observed, the deformation of the cohesive sediment around the base of the plant is a result of to-and-fro movement. This deformation cavity gives the seedling progressively more space

for movement under the to-and-fro motion of the waves. A consequence of this increasing motion freedom is that the lateral plant roots are progressively pried out of the sediment or broken. This exposes the roots to the waves and the constant movement loosens the sediment around these lateral roots making the sediment holding these roots in place easier to erode. The effect is that the plant has even more space to move and the roots that are holding the plant upright are slowly losing strength and anchorage. The anchorage loss causes the seedlings to topple under extended

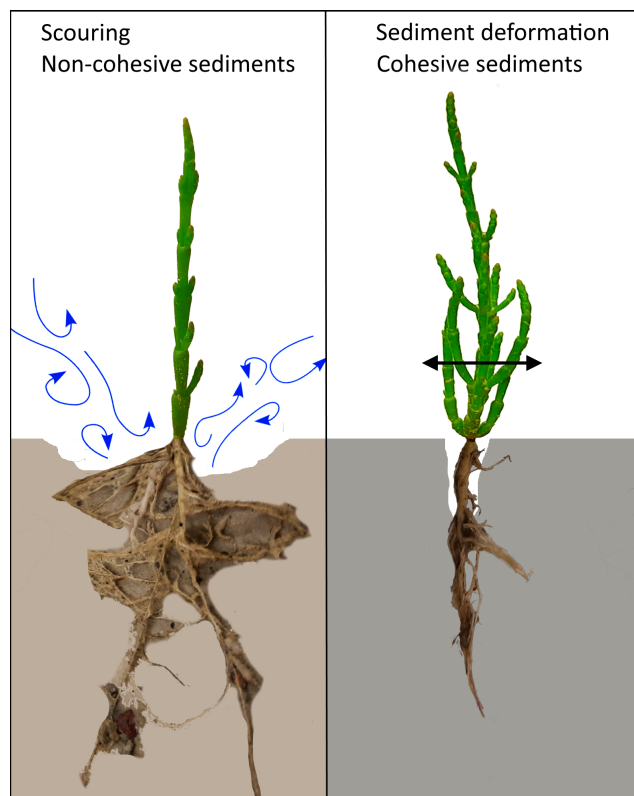


Figure 3.18: Depression forming process in non-cohesive sediment (left) and cohesive sediment (right)

wave loading; the seedling will thus have failed. However, the seedlings will not flush away because the deeper part of the root is still anchored securely in the soil. The failure mechanisms in cohesive and non-cohesive sediments are illustrated in figure 3.19. In this figure, each mechanism is divided into four stages.

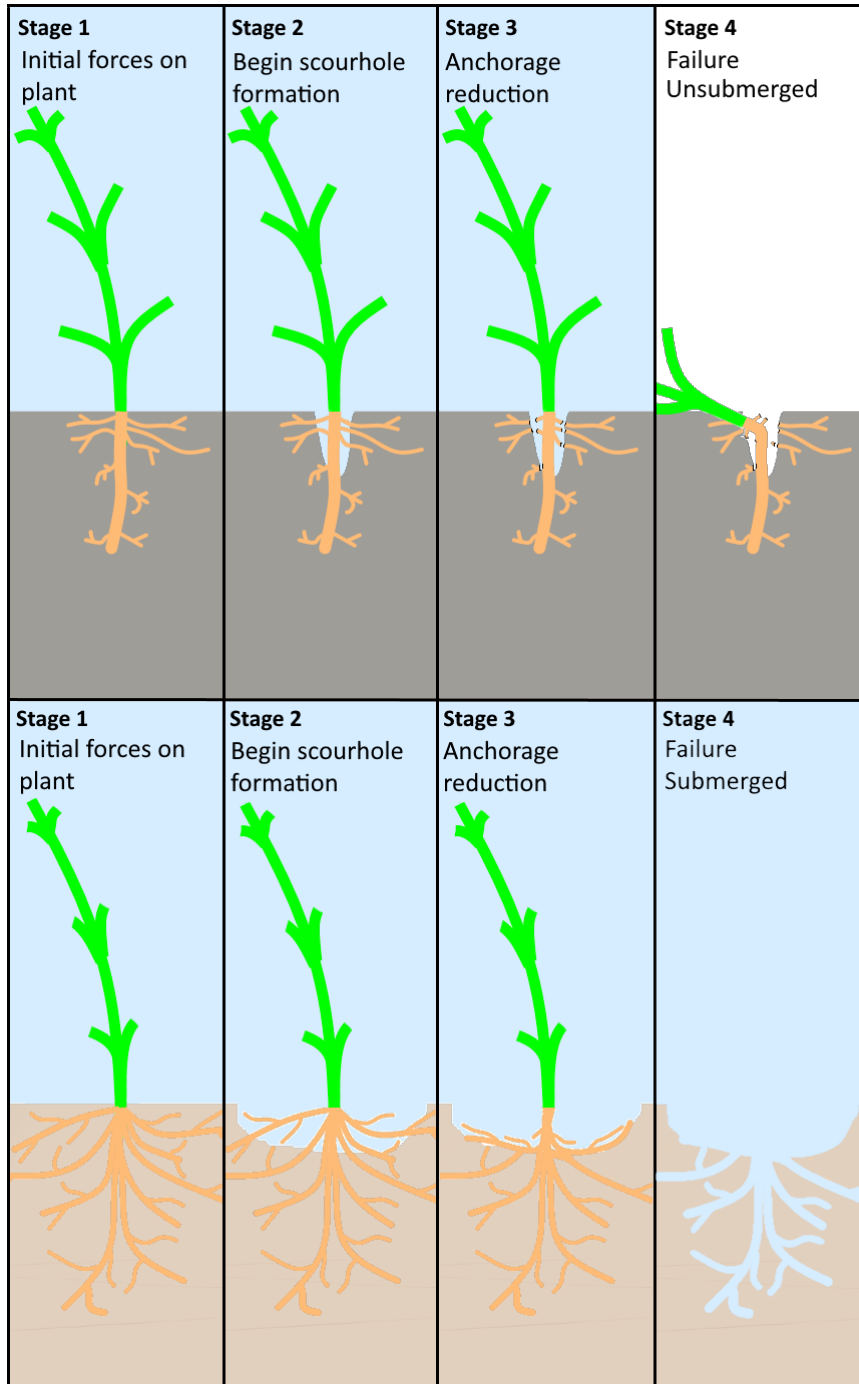


Figure 3.19: The 4 stages of failure of *Salicornia* seedlings in mud and sand. Stage 1: the initial forces on the plant. Stage 2: start of depression development around plant, narrow and uneven in mud, wide and smooth in sand. Stage 3: roots begin to lose anchorage. Stage 4: plant has failed, flushed away in sand and toppedled in mud.

3.5.1 Stage 1: initial forces on seedling

Initially, the forces on the above and belowground biomass do not act directly along the same line of action (Figure 3.20A). Therefore the forces that are applied to the seedlings do not pass through the centroid of the body. This causes the plants to have a moment resultant, which means the plants will rotate or tilt. This effect is illustrated by figure 3.20B. The plant will rotate around the point where the root enters the soil, the pivot point. Once the plant has tilted, and the forces applied on the seedlings do pass through the centroid of the body, the tilting will stop and the plant is in balance (Figure 3.20C). In the experiment, the seedlings in mud (of different

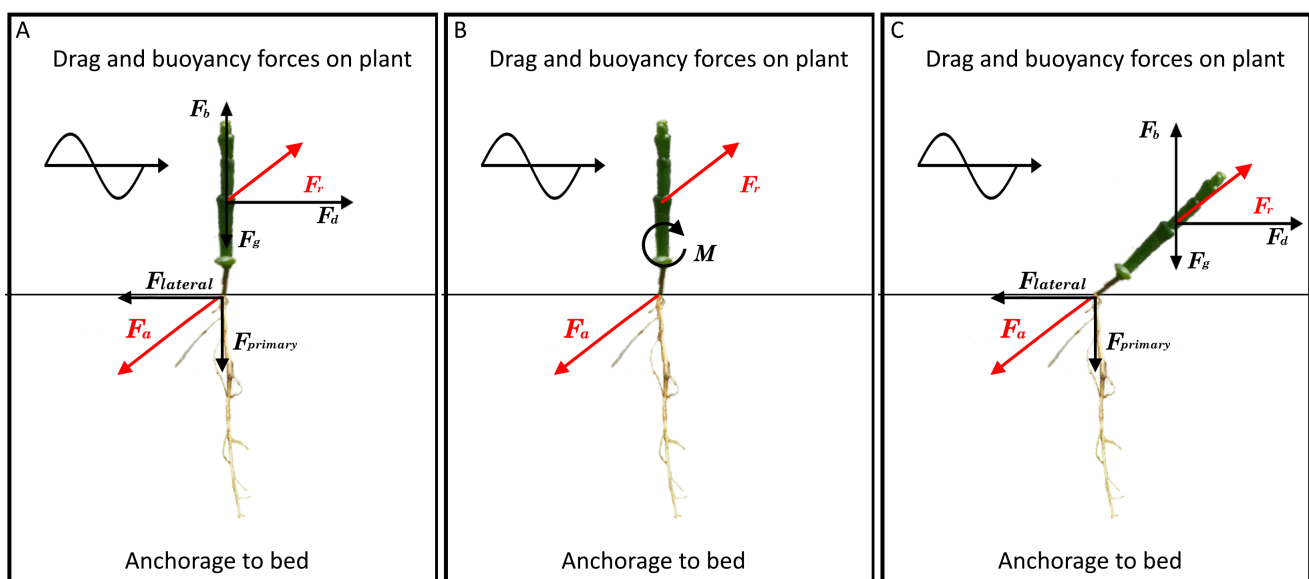


Figure 3.20: A:initial forces on seedling (left), B:Resulting moment forces on seedlings (middle), C:Tilt of plant due to moment forces (right)

ages) had larger stem diameters than their counterparts in sand. This trend was also visible for the frontal surface area. Therefore, on average, plants growing in mud will experience higher buoyancy and drag forces under equal wave conditions compared to plants in sand. In the flume, the aboveground biomass experiences drag and buoyancy forces representing the uprooting forces (F_r) on the plant, causing failure. Conversely, the belowground biomass provides the anchorage of the seedling to the bed and prevents failure of the plant.

Another force that acts on the plant, is the force due to momentum carried by the plant. However, because the low weight of the plants (less than a gram) and moderate flow velocities, this force is several orders of magnitude smaller than the drag forces acting in the same direction. The jerk number is therefore also very small and thus, this force is neglected in this study.

The plant anchorage depends on the properties of the plant's root system, the sediment characteristics and a dimensionless specific attachment coefficient (k). The dimensionless attachment coefficient is dependent on the type of vegetation. The k value for *Salicornia* is 6.5; for the full calculation, see appendix C. When the soil strength and the root area of a seedling are known, this can be used to calculate the theoretical anchorage.

3.5.2 Stage 2 and stage 3: begin and development scour-hole

Figure 3.21A represents the forces at the beginning of the scour-hole formation. Due to the scour-hole development, the pivot point of the plant moves down along the root (Figure 3.21B). This increases the lever arm of the force's action on the above biomass of the plant, thus the moment balance shifts. Furthermore, a part of the plant root can no longer assist in anchoring the plant and has more space to move. After a period of exposure to the waves, the anchorage of the seedlings to the

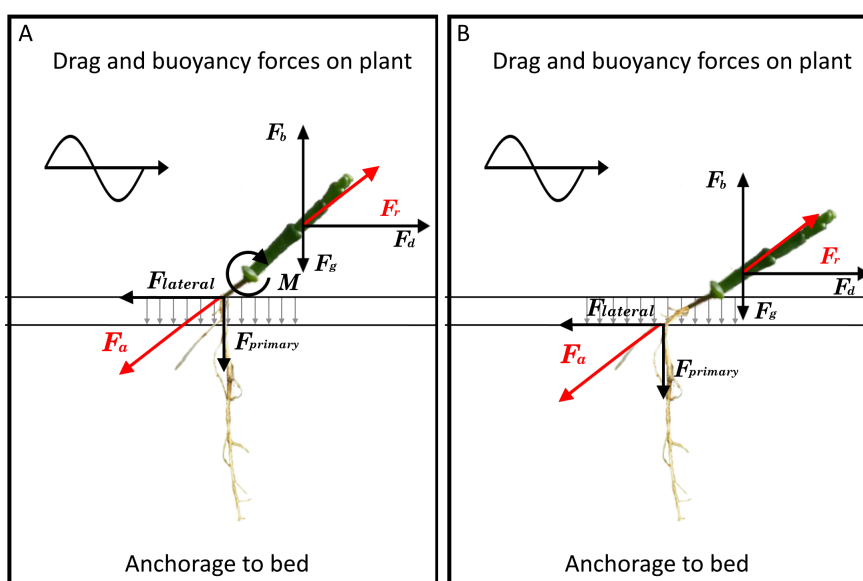


Figure 3.21: A: Begin scour-hole formation (left), B: Development scour-hole (right)

bed decreased. In the wave flume, several mechanisms that cause the plants to lose anchorage were observed. The soil around the roots of some seedlings eroded; this left the plant roots with less material for support and anchorage. Furthermore, the roots of some plants were damaged or broken by the wave loading, so the plant had fewer roots for anchorage.

An important observation was that the shallow roots near the stem had the most considerable contribution in keeping the plants upright. So losing anchorage from

the upper roots has more consequences for the plant regarding toppling than the loss of deeper roots.

In figure 3.22 and 3.23, the difference in depression-hole development between cohesive and non-cohesive soils is presented. Overall around plants in sand more profound depression-holes developed (2.5 times deeper on average) in the same amount of time. The in sand also plant received less wave energy and flume time compared to mud. Another observation from the flume experiment was that the shape of the scour in sandy sediment is very different compared to mud. In sand, the scour-hole was very wide and the transition from the regular bed to the scour-hole smooth. In mud, the depression around the plant was narrow, chunky, and very asymmetrical.

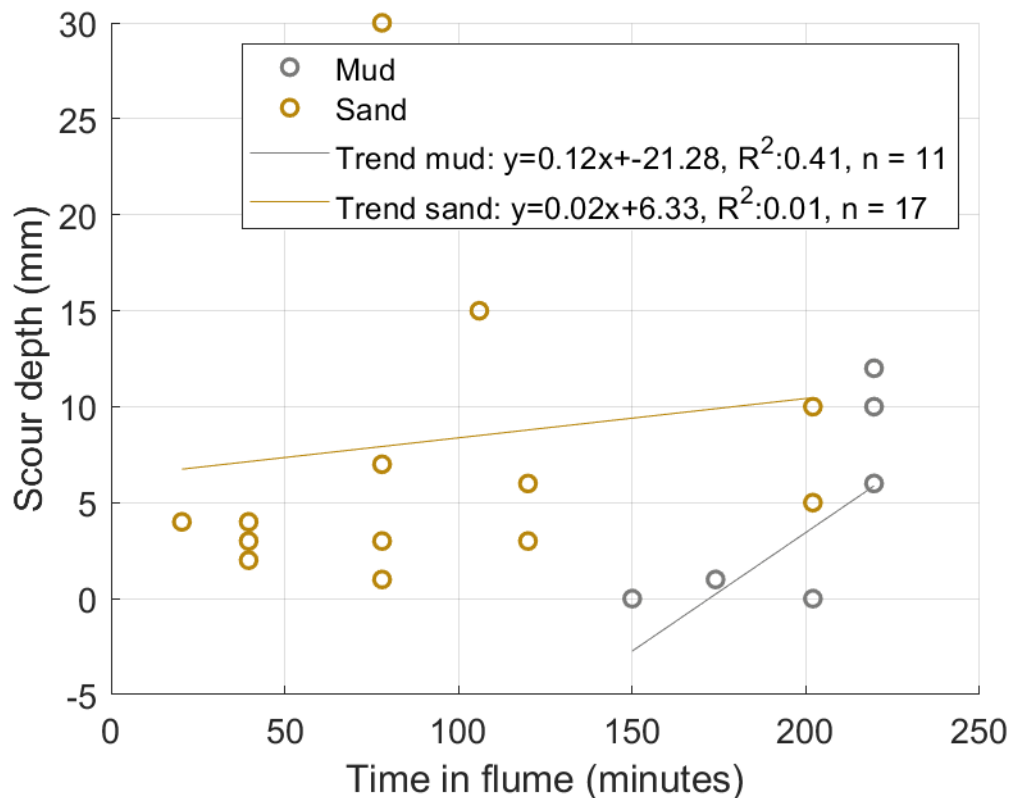


Figure 3.22: Scour-hole depth development with total cumulative time in flume in sand and mud

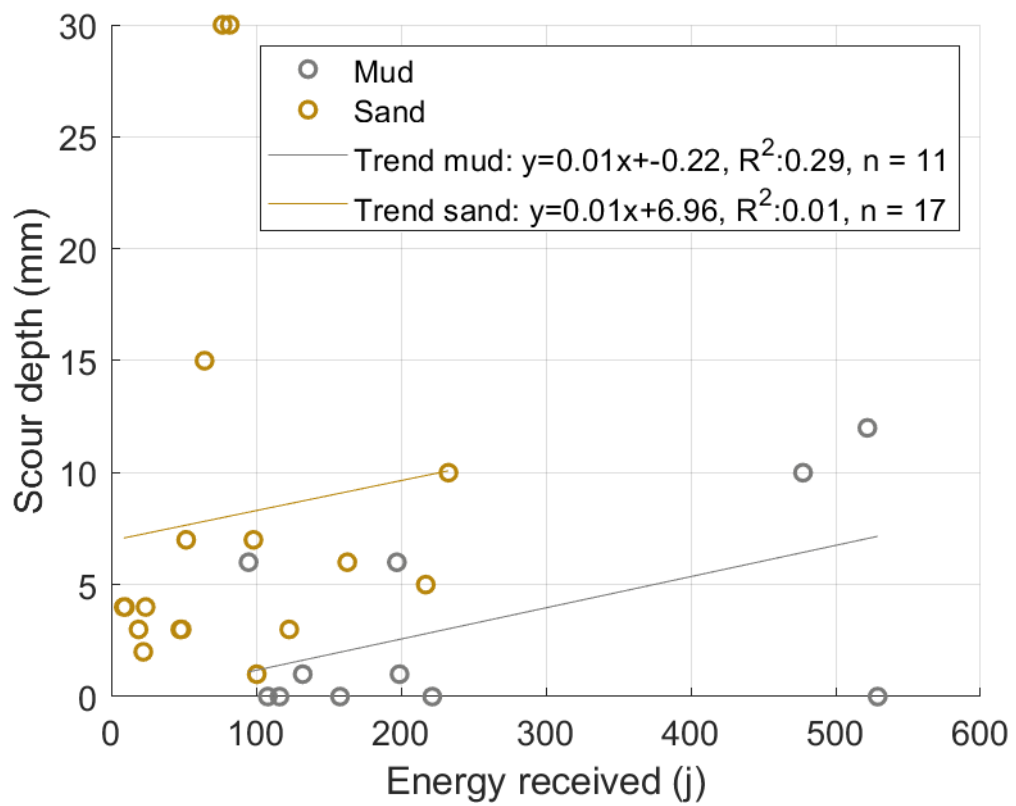


Figure 3.23: Scour-hole depth development with received amount of energy in flume in sand and mud

3.5.3 Stage 4: failure of the plant and behaviour once failed

Once the equilibrium between the uprooting and anchoring forces is disrupted, the seedlings will fail. The observed failure of the seedling in sand was very different compared to mud. In sand, the seedlings flushed away when still submerged (Figure 3.24A). Seedlings growing in mud toppled under extended wave loading, but did not flush away entirely, because the deeper part of the root was still anchored securely in the soil (Figure 3.24C). Furthermore, because of the buoyancy forces on the seedlings in mud, the plants will remain upright when submerged. Once the plants are unsubmerged, the buoyancy forces disappear and the only force acting on the plants is the gravity force produced by the seedling's own mass (Figure 3.24B). If the root and stem can counter these moment forces, the plant will remain upright; otherwise, the plant will fail. Sediment deformation can reduce the anchorage of the root. Another consequence of sediment deformation is that the seedlings have more room to move and tilt. This tilt also increases the lever arm of the gravity force. So the moment produced by this force will also increase and put even more stress on the roots and stem.

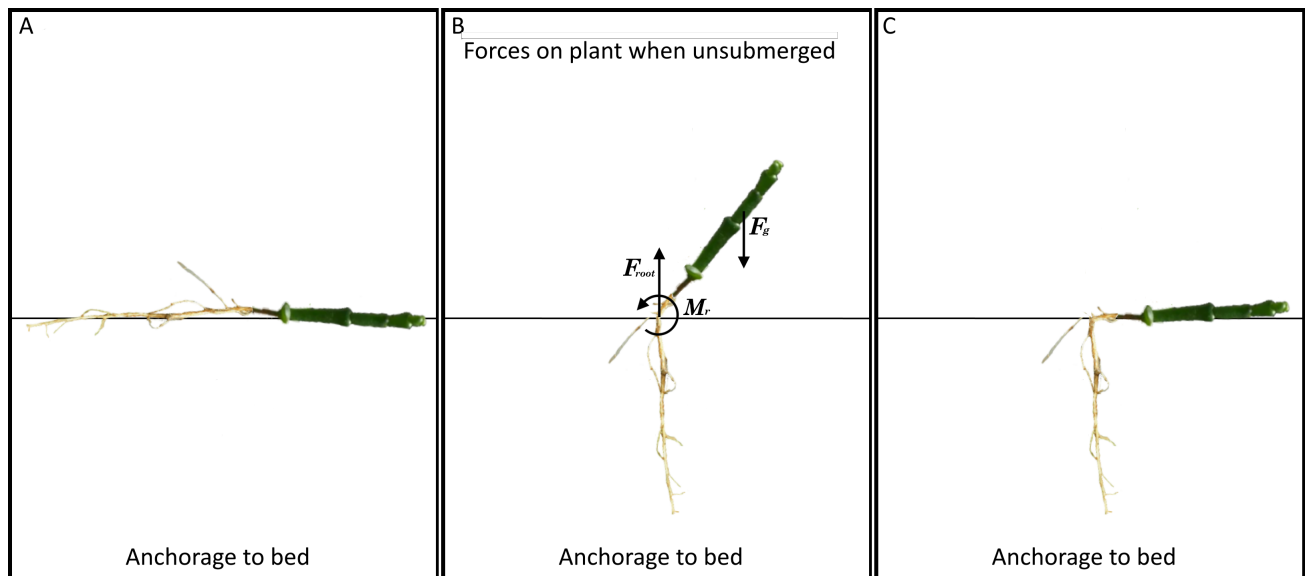


Figure 3.24: A: Submerged failure in sand (left), B: unsubmerged force balance of a seedling (middle), C: unsubmerged failure in mud (right)

3.6 Thresholds of the failure of *Salicornia* seedlings

The thresholds for failure of a *Salicornia* seedling during the WoO2 window are dependent on the bio-morphological parameters of the plants, as well as the wave conditions. For the determination of the thresholds, plant averages observed during the experiment were used. The thresholds were divided between non-cohesive and cohesive sediment. Section 3.6.1 presents the thresholds in non-cohesive sediment. Section 3.6.2 presents the thresholds in cohesive sediment.

3.6.1 Failure thresholds in non-cohesive sediments

In non-cohesive sediments, erosion is the dominant process in the failure of a seedling. During the experiment, plant failure occurred when a scour-hole due to erosion reached a depth of approximately 17% of the root length. The volume of the root system can be describe as hemisphere. So a reduction of 17% in root length equals a loss of root volume of 26%. To reach this depth, the plants received on average 8.5 joule of wave energy or 14 minutes of adjusted flume time per mm decrease.

For the critical erosion depth (CED) in sand, only 2 to 3 data points per age group where available so this gave large differences in CED between the age groups, even though the maximum difference in age between the groups was 15 days (Figure 3.25). The average CED over all ages was 9 mm.

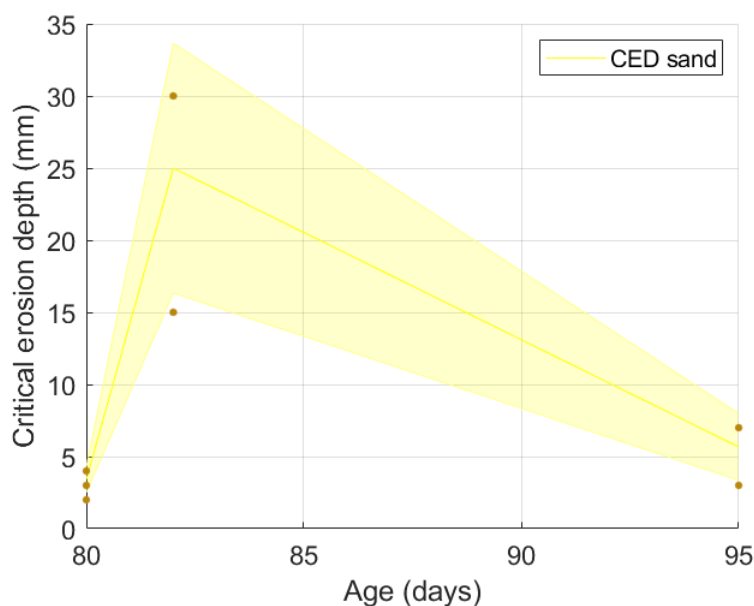


Figure 3.25: Critical erosion depth over different age groups, average with standard deviation band

3.6.2 Failure threshold in cohesive sediments

In cohesive sediments, the to-and-fro motions of the plants in the flume are the primary process, that induces deformation around the plants. The threshold is the amount of to-and-fro motions of a certain magnitude a plant can endure before failure. These motions are countered by the number, thickness and length of the lateral roots of the seedlings. So there is a relation between the root system of a plant, the amount of to-and-fro motions, and the plant's failure.

However, due to the limited amount of seedlings that failed ($n \leq 5$) in mud during the flume experiment, the exact amount of to-and-fro motions of a certain magnitude a plant can withstand before failure and the relation to the root characteristics could not be determined. So due to lack of data, the failure thresholds could not be determined, figure 3.26 and 3.27 do however suggest that there is a positive relationship between the belowground plant traits (root length and root thickness) and the amount of to-and-fro motions a plant can endure.

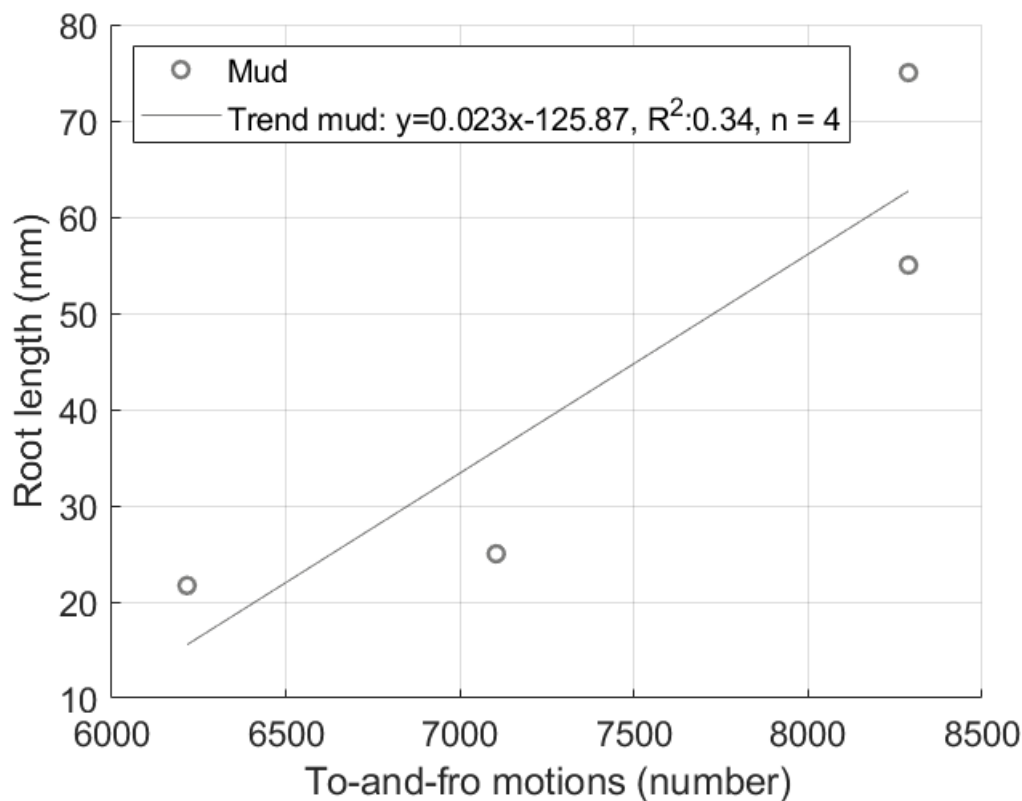


Figure 3.26: Number of to-and-fro motions until failure compared to root length of the seedlings

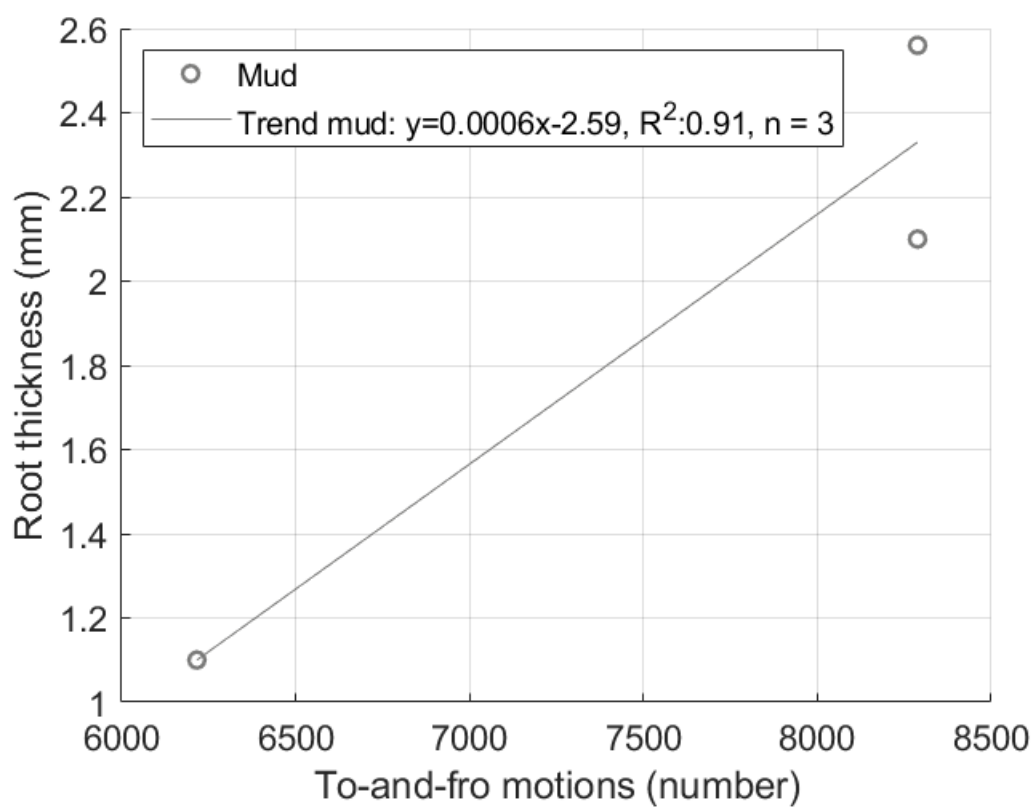


Figure 3.27: Number of to-and-fro motions until failure compared to root thickness of the seedlings

3.7 Expanse of the WoO framework

This research found that, in cohesive sediment, erosion was not the dominant process that induced failure in *Salicornia* seedlings. Thus, CED may not be the best approach for determining the establishment of saltmarshes with a high mud content. So in this research, the WoO framework is defined in terms of BSS instead.

During the flume experiment, seedlings growing in cohesive sediment could withstand more wave loading compared to seedlings in non-cohesive sediment. So this research suggests that seedlings growing in sediments with a high clay content have a more flexible WoO2 window (the critical BSS (τ_{veg}) is larger in mud) (Figure 3.28, Scenario B). Furthermore, in clay that is consolidated, with high soil strength, seedlings had an even more flexible WoO2 (Figure 3.28, Scenario D). However, an intervention increasing consolidation most likely negatively affects successful salt marsh establishment, when implemented before seedlings have completed the WoO1 window (Figure 3.28, Scenario C). In consolidated clay slower root elongation and reduced root length was observed. Slower growing roots in this first phase expands the duration of the WoO1 window and can thus negatively affect successful salt marsh establishment.

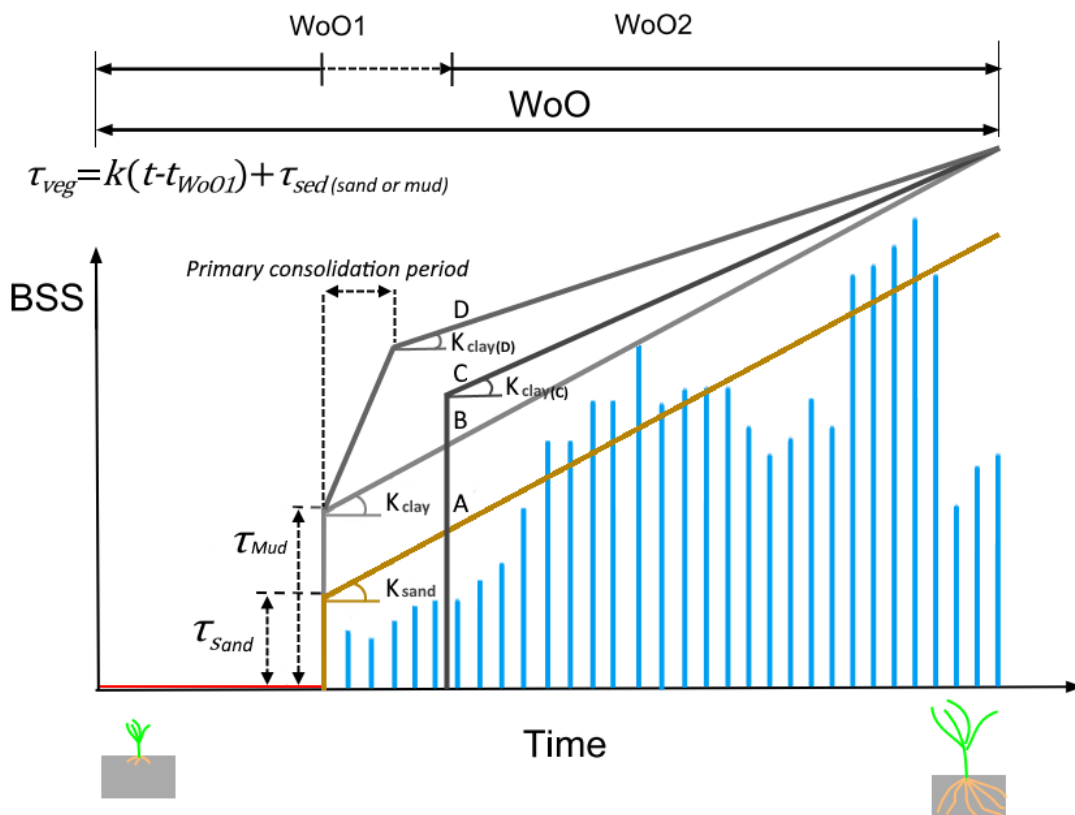


Figure 3.28: Schematization of the WoO adapted from Hu et al., (2015). A,B,C and D are different scenarios for vegetation establishment

- A. A scenario of the establishment of vegetation on a salt marsh where the sediment consists primarily of non-cohesive sediment.
- B. A scenario of the establishment of vegetation on a salt marsh with a high clay content where the clay does not experience increased consolidation due to an intervention. The higher erosion resistance and soil strength of the cohesive sediment will result in a more flexible WoO2 window for vegetation establishment.
- C. A scenario of the establishment of vegetation on a salt marsh with a high clay content where the cohesive sediment was already consolidated before the WoO1 window was initiated. In this scenario, the WoO1 is longer because the initial anchorage of the seeds takes longer, because of the high soil strength. This soil strength also means that once anchored, the seedlings will not easily flush away due to erosion.
- D. A scenario of the establishment of vegetation on a salt marsh with a high clay content where subsequently to the conclusion of WoO1, an intervention is implemented that induces consolidation of the sediment. During the primary consolidation period, the soil strength of the salt marsh sediment rapidly increases and so does the plant anchorage.

Discussion

This chapter starts discussing the methods and practises of the flume experiment in section 4.1. This is followed by sections 4.2 and 4.3, discussing the findings of this research. In section 4.4, the irregular waves observed during the experiment are compared to simulated regular waves and in section 4.5 a simple model describing seedling failure is discussed. In section 4.6, the practical implications of the research are considered.

4.1 Methods of the flume experiment and observations

During the growing phase of the flume experiment, the different batches with seedlings displayed considerable variation in plant characteristics. The samples from the first batch for example, on average lower had plant heights. This stunted growth was presumably the result of extreme weather during the growing phase of this first batch. Extreme weather is part of the environmental factors influencing the development of vegetation on salt marshes. The extreme weather conditions also resulted in seedling death and thus loss of data. In the experiments of Bouma et al. (2016), Cao et al. (2018), and D. Poppema (2017), the plants were grown in tidal mesocosms with a constant temperature. So in these experiments, the seedlings were exposed less to the natural environment and varying climate conditions. The research of Bouma et al. (2016), Cao et al. (2018), and D. Poppema (2017) also used the tidal mesocosm to expose the plants to a semi-diurnal tide. This is another difference compared to this research in which the plants were irrigated bidaily. Because the plants were not inundated regularly, waves and currents were absent during vegetation growth. This is a substantial difference from vegetation growth in the field. The presence of waves and currents in the field may influence the growth and biomorphological development of the seedlings.

Furthermore, during the flume experiment, the extraordinarily hot weather in combination with a low moisture content resulted in strongly consolidated clay samples, with uncharacteristically high soil strengths. The research of Gillen et al. (2020) found that soil shear strength in monospecific salt marshes ranged from 5 to 36 kPa. Soil strengths between 15.30 kPa and 68.40 kPa were measured during the flume experiment. This is a higher range than a typical salt marsh. Due to these high soil strengths, and in extension, high root anchorage values, the samples may not accurately have represented conventional natural conditions. For the comparison with plants in the field, plants that originated from the Marconi site near Delftzijl were also tested in the flume. These tests using field plants failed, however. The plants and a portion of original sediment were embedded in the boxes and did not lose anchorage but were flushed out together with the original sediment.

During the experiment, some of the plant and sediment traits that could have been useful for the determination of the root anchorage, were not documented. For example, the dry weight of the root system or the characteristics of the lateral roots were not documented. Some of these plant traits were estimated subsequently using the photos.

This does, however, add uncertainty to the measurement; the photo needs to be scaled and is only 2D, so some of the lateral roots might not be visible in the photo. Furthermore, the exact thickness of the roots was hard to determine on the photos because of the sediment clinging to the roots.

As regards to the sediment characteristics, the shear vane used for the experiment was not sensitive enough to measure the shear strength (<0.22 kPa) of some of the fresh mud samples. So the shear strength of these samples could not be determined. The most sensitive shear vane used was an “extra-large” shear vane (80x100 mm) and had a multiply factor of 0.025. For the fresh mud samples, a slightly more sensitive vane is recommended. Furthermore, sediment samples of each box were sent to a lab for analysis. These samples got lost however, so they could not be used. The results from the analyses could, for example, have been used to determine the density of the sediment in the different boxes or to determine the moisture content. These parameters are essential for the erosion calculation (equation 1.2) and give more insight into the consolidation process.

4.2 The biophysical plant parameters

This research found that the sediment type considerably influences the belowground biomass of *Salicornia* seedlings. In non-cohesive sediments, the roots were long and thin and in cohesive sediments relatively short and thick. This is because the root system growth and the elongation of individual roots are often limited by soil strength (Mickovski, 2003), and roots have evolved ways of penetrating and exploiting compacted soils. For example, the thickening of the root relieves stress in front of the root apex and decreases buckling because the stress is distributed over a larger volume (Bengough et al., 2006). So sediments with higher compaction and soil strength, like the cohesive sediments in this study, will limit root elongation and induce thickening of the roots.

The observed aboveground differences in plant morphology, namely the complexity of the plants, are likely driven by the larger water and nutrient availability in cohesive sediments, in comparison of the less fertile non-cohesive sediments used in the experiment. Prof. L. Mommer from the Wageningen University Research confirmed that this was likely the reason for the differences in plant growth.

The measured removal force of the seedlings during the experiment, was significantly higher than the values measured at the Marconi site by the research of Hendriks (2020). The degree of consolidation of the material, and in turn the higher soil strength of the samples, is a probable cause for this difference. Furthermore, the plant-specific attachment parameter (Schutten et al., 2005) that was used to determine the anchorage of the seedlings, was calibrated using the removal forces and soil strengths measured during the flume experiment. In the equation of the anchorage force, the high soil strength of cohesive sediments is compensated for. However, when the plant-specific attachment parameter of *Salicornia* is used in future research, it may be prudent to recalibrate the parameter. Especially because the parameter in this research is calibrated using a relatively low number of observations ($n=5$), so calibrating with more samples will increase the accuracy.

4.3 Erosion and consolidation of sand-mud mixtures

In the growth phase of the experiment, the consolidation rate of the cohesive sediment was high in the beginning (the primary consolidation phase), but flattened out over time (secondary consolidation phase). A typical duration for the primary consolidation phase is 10 to 50 days; the primary consolidation phase observed in the experiment occurred well within this range (Figure 4.1). The soil strength is di-

rectly related to the consolidation degree of the sediment (Germaine et al., 1998). Therefore, consolidation of the cohesive sediment increases the erosion resistance. Furthermore, cohesive sediments typically have higher soil strengths compared to non-cohesive sediments (Schoutens et al., 2021). Thus, sediments with increasing clay content exhibit higher erosion resistance (Houwing, 1999; Kothiyari et al., 2014). During the flume experiment. This effect of consolidation on erosion resistance was also observed; Mud that had settled for only one day, with little consolidation, eroded easily and

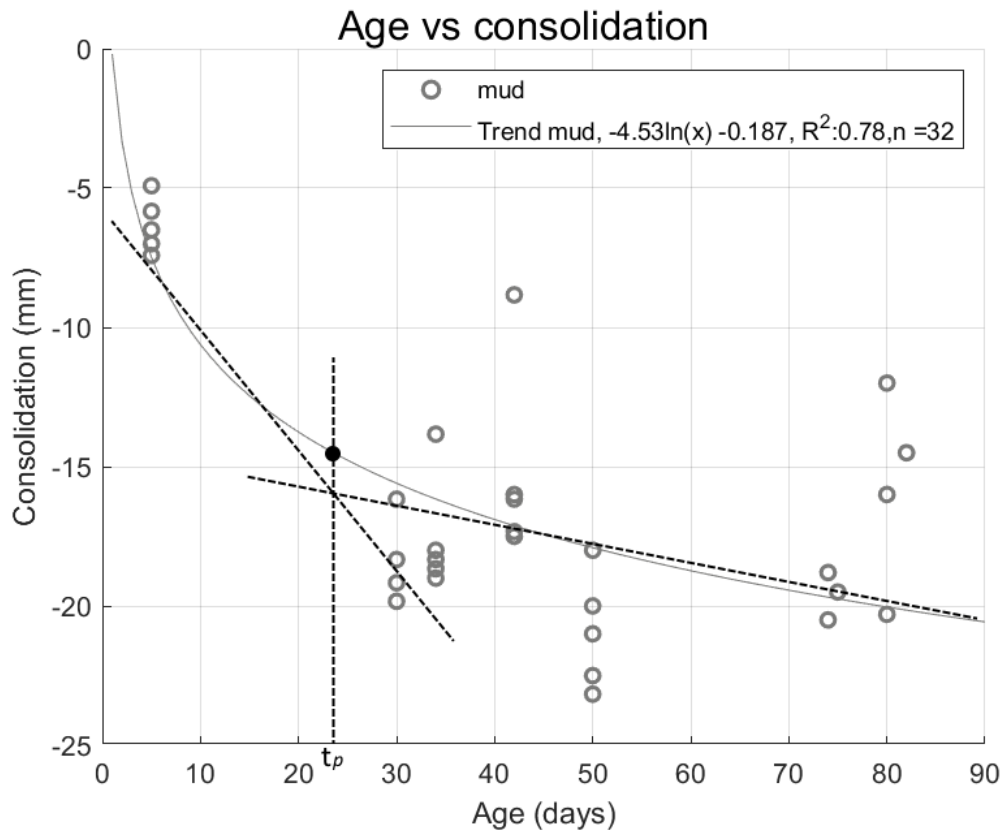


Figure 4.1: Division of the primary and secondary consolidation of the Zuidgors sediment

did not reach an equilibrium. Mud that had settled for five days eroded slower and eventually reached an equilibrium erosion depth (Figure 3.2). The top layer of this five-day-old mud was, however, still easy to erode. The sediment seemed to be stratified, with an easy to erode top layer and a layer beneath this where the erosion resistance was higher. The research of Perera et al. (2020) also used this two-layer concept which distinguishes between a more easily erodible surface aggregate layer (simulated using a linear erosion model) and an underlying sediment layer bound by both the physio-chemical cohesion and biological adhesion. The stratification is also the reason why there was not a good trendline that incorporated both layers. There-

fore, in figure 3.2, the first part of the trendline that incorporated the top layer of the sediment was left out. The research of Kranenburg and Winterwerp (1997) also noted the gradual increase in bed strength with depth, which is related to the increase in bed density.

The research of Onorato et al. (2006) observed that the development of scour-holes also occurs at a slower rate in cohesive sediments than in non-cohesive sediments. This corresponds with the observation during the flume experiment that scouring was limited or even non-existent in cohesive sediment. This was to be expected, because scouring is an erosion process (Schoutens et al., 2021) and will thus be affected by the higher erosion resistance of the cohesive sediment. Highly cohesive sediments have a high shear strength, which prevents erosion (e.g., scouring) and potential uprooting, even under storm wave conditions (Möller et al., 2014; Spencer et al., 2016).

The research of Jacobs (2011) related the different erosion modes of sand-mud mixtures to the bed shear stress and the shear strength of the bed (e.g., surface erosion, floc erosion and mass erosion). Figure 4.2 gives an overview of the classification of erosion modes for cohesive soils with the bed shear stress as a function of the bed strength. During the flume experiment mainly a stable bed was observed and some surface and floc erosion in the cohesive sediment samples. This is compared to the erosion modes that should occur according to the classification graph of the research of Jacobs (2011), using the bed strength measured during the flume experiment and the shears stresses produced by the irregular waves. The maximum bed shear stress produced in the flume was 0.81 Pa; the shear strength from the cohesive sediment samples (including the fresh mud) ranged from 0.50-68.40 kPa or 500-68400 Pa. It should be noted that some of the fresh mud samples had lower shear strengths. According to the graph, some floc and surface erosion should be visible at the low end of this range, this is in the fresh mud, this is in accordance with the observations in the flume. Nevertheless, according to the classification graph, the bed should be mostly stable, especially at the higher shear strengths, which was again what we observed in the flume.

4.3.1 Erosion and sediment transport during short storm events vs longer moderate events

In non-cohesive sediment, most sediment transport occurs during moderate events (Leonardi & Fagherazzi, 2015); an extended period of moderate waves will produce more erosion and will influence failure more than a short storm event. However, in

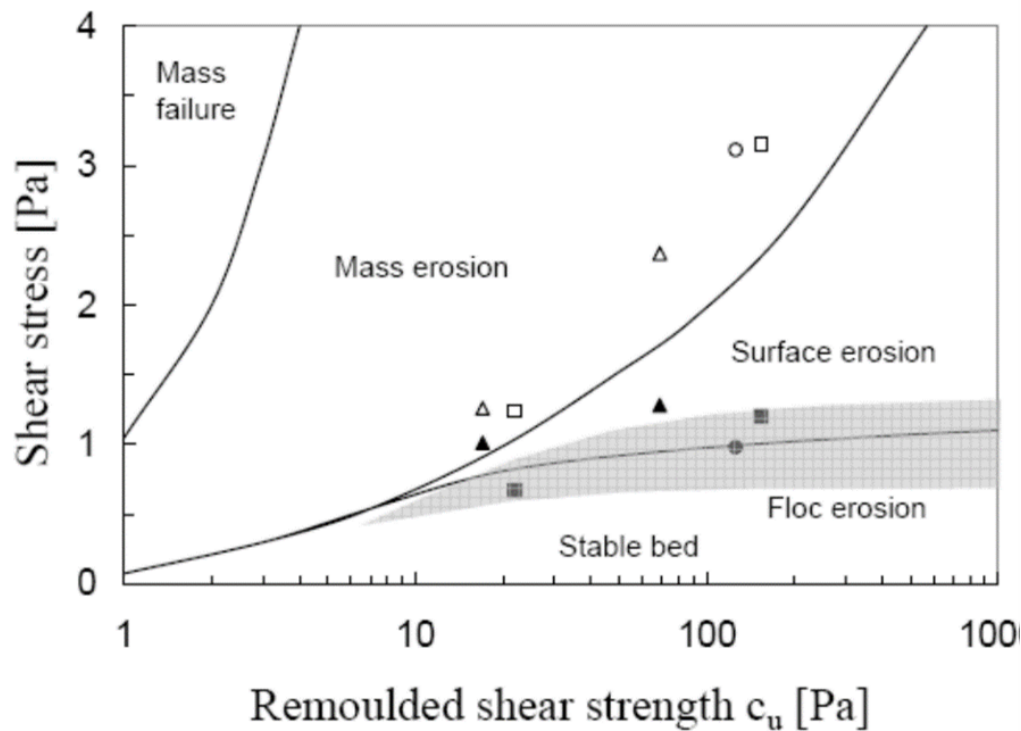


Figure 4.2: Classification of erosion modes for cohesive soils with the bed shear stress as a function of the bed strength (Jacobs, 2011)

cohesive sediment, the critical bed shear stress is much higher, so moderate events will not cause much erosion. A substantial storm event however, might produce bed shear stresses necessary for sediment transport. In cohesive sediment, the to-and-fro motion of the plant is instrumental for failure. Plant roots have evolved to withstand some motion, so moderate events causing limited to-and-fro motions probably will not induce failure. In cohesive sediment, during storm events, the stresses on the roots are larger because the to-and-fro motions are more pronounced; this may exceed the limits of force the roots can withstand and result in failure. So, in cohesive sediment, a short storm event might be worse for the plants than in non-cohesive sediment.

4.4 Irregular vs regular waves

The significant wave height (H_s) is commonly used in engineering design considerations as a representative wave to approximate the otherwise irregular wave field, and seems to correlate well with visual estimates of wave height from experienced observers (Young, 2017). Figure 4.3 shows the flow velocities produced by the irregular waves ($H_s=0.2$ m; $T=2.5$ s) observed during the flume experiment. The

waves of a monochromatic wave spectrum ($H=0.2$ m; $T=2.5$ s) with comparable wave characteristics in an equal time interval (Figure 4.3) produce lower maximum flow velocity peaks (0.39 m/s) compared to the irregular waves (0.82 m/s). However, about 77% of the peaks in the irregular wave spectrum are lower than the peaks of the monochromatic wave spectrum. During the experiment, the irregular waves produced short intense periods of flow velocity peaks and flow direction oscillations, and long calm periods compared to monochromatic waves, in which all peaks were equal (Figure 4.4). These higher flow velocity peaks can have a major impact on plant failure and erosion.

The drag forces on the seedlings are proportional to the square of the flow velocity (Equation 2.1), so the flow velocity peaks produced by the irregular waves result in significantly higher maximum drag forces on the plants compared to the maximum drag forces produced by the regular waves. The roots providing anchorage of the plants have to counter these higher drag forces. Thus plants may fail in a shorter period of wave loading under irregular waves than under regular waves.

The induced erosion, also differs between irregular and regular waves. Approximately 70% of the bed shear stress peaks produced by irregular waves were lower than the peaks of the monochromatic wave spectrum. However, the 30% of the peaks that were higher, were often two to three times higher. Especially in cohesive sediment these higher peaks might impact erosion and plant failure. The non-cohesive sandy sediment had a critical bed shear stress of 0.14 Pa, so sediment transport should occur for both wave types, although monochromatic waves will cause consistent transport and the irregular waves will cause periods of hardly any transport and periods with a high sediment transport rate. The cohesive Zuidgors sediment had a critical bed shear stress of 1 Pa. The monochromatic waves are not able to erode the cohesive sediment; the critical bed shear stress far exceeds the maximum bed shear stress produced by these waves. So, the monochromatic waves could not erode the cohesive sediment and cause anchorage reduction in the seedlings. Irregular waves are, however, able to erode the sediments during periods with high flow velocity peaks. The irregular waves observed during the experiment were able to produce bed shear stresses that can result in sediment transport of the cohesive sediment and might reduce the anchorage of the plants but only during the short periods of high bed shear stress.

In the research of D. W. Poppema et al. (2019) the plants were exposed to five regular waves of a certain wave type to test how much erosion the plants could withstand. When studying (five) irregular waves with a comparable significant wave height, it is hard to compare the results because of the random nature of these waves

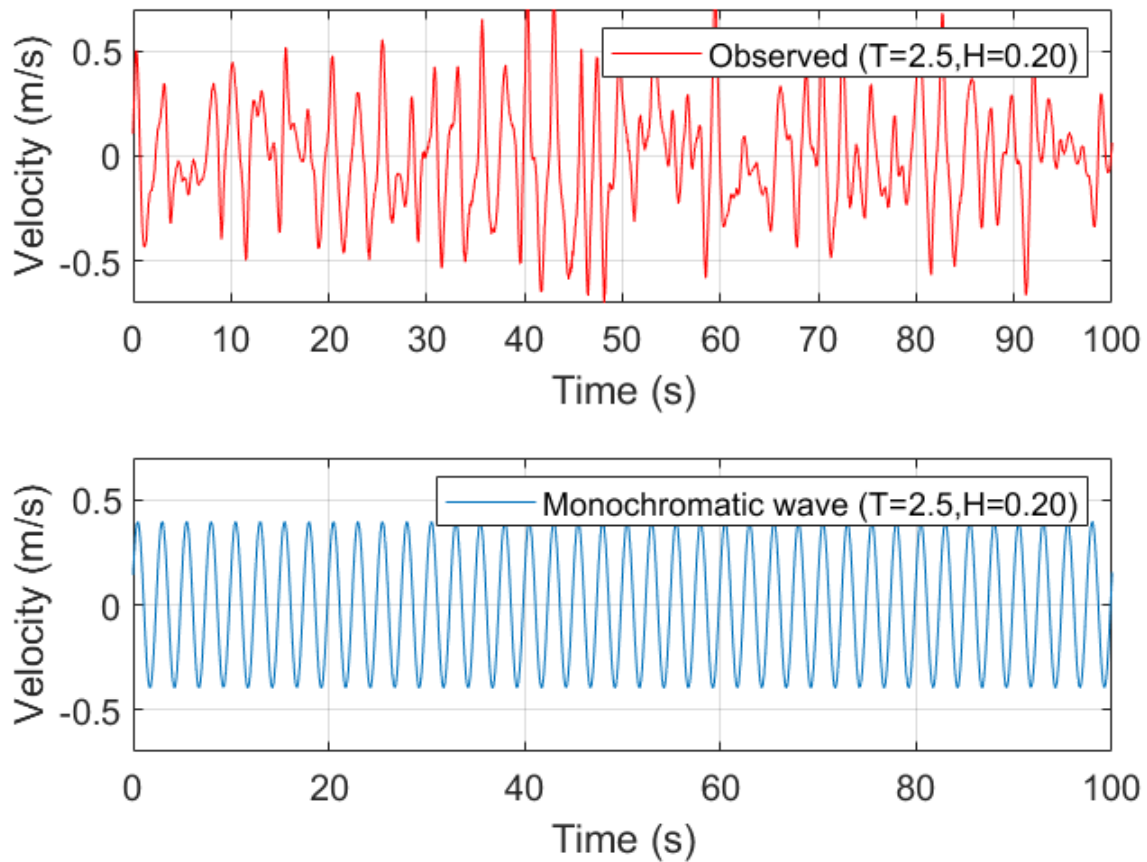


Figure 4.3: Flow velocities observed in the wave flume produced by an irregular waves (top), flow velocities produced by waves of a monochromatic wave spectrum (bottom)

(which depends on the wave spectrum). For the comparison of irregular and regular waves, looking at waves with similar wave energy might be a better alternative, as performed in the research of Faraci, (2002). Another alternative is assuming that the plants fail at the largest peaks of the irregular wave spectrum and comparing the five largest peaks of an irregular wave spectrum to five peaks of a monochromatic wave spectrum in respect to plant failure and erosion.

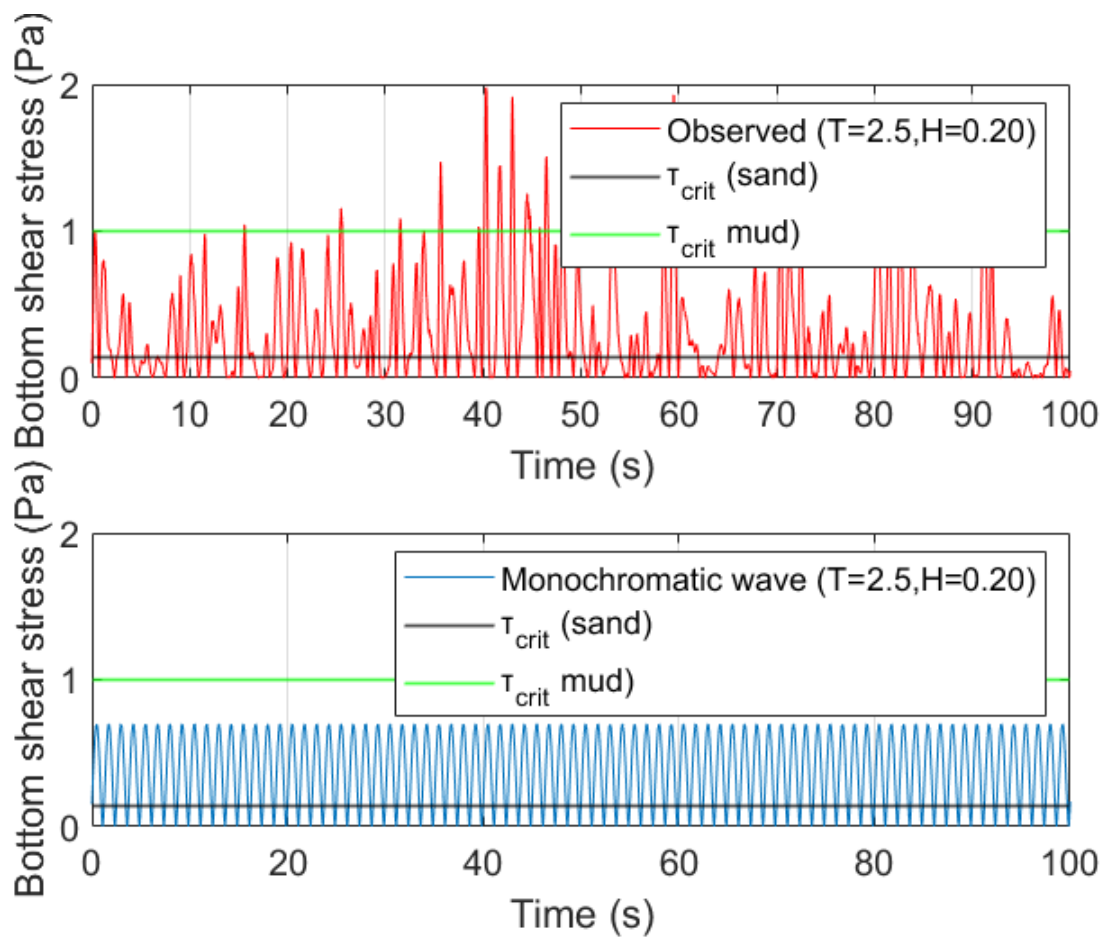


Figure 4.4: Bed shear stress produced by the irregular wave observed in the wave flume (top), bed shear stress produced by waves of a monochromatic wave spectrum (bottom), T_{crit} is the critical bed shear stress of the respective sediment type

4.5 Seedling failure

The failure mechanisms observed in the flume, were elaborated using force balances. The balances describe the theoretical forces subjected to the plants. Failure of individual seedlings depends on the equilibrium between the vectorial sum of the buoyancy together with drag and momentum forces of the waves on the above-ground biomass and the resistance due to root anchoring. So a plant will fail, once the buoyancy (F_b) minus the gravity force of the plant (F_g) together with the drag force (F_d) and momentum force (F_m) exceed the resistance due to root anchoring (F_a). All individual equations for these forces (Chapter 2) together result in a simple model for failure (Equation 4.1 and 4.2)

$$\text{failure when } F_a < (F_b - F_g) + F_d + F_m \quad (4.1)$$

$$\underbrace{k * A_r^{\frac{2}{3}} * C_u}_{F_a} < \underbrace{(\rho_w * V_{plant} - m_{plant})}_{F_b - F_g} * \underbrace{g \frac{1}{2} C_D \rho_w \emptyset_{stem}(z) U^2}_{F_d} + \underbrace{m * \frac{dv}{dt}}_{F_m} \quad (4.2)$$

Under wave action, the buoyancy and gravity forces on the plants are constant because these forces are primarily dependent on the aboveground plant traits of the seedlings and these plant traits will not change much in the short period in the flume. However, due to the varying tilts of the plants, the lever arm will vary over time, so the moment these forces exert is changing over time. Therefore, these moments need to be countered by the plant's roots and put more stress on the roots.

The forces on the plants with most variation, are the drag forces and the root anchorage. Drag forces vary strongly over time and direction when waves pass over the plants. The anchorage slowly reduces over time due to scouring and prying out of the roots; this process varies with the different sediments. The plants will most likely fail at a flow velocity peak once the anchorage has reduced over time and can not counter these forces anymore. The anchorage reduction is a cumulative process over time. The drag force peak is a snapshot at a certain moment.

The model for plant failure (equation 4.1) might be oversimplified, especially in cohesive sediment in which erosion is not the dominant process reducing anchorage. The process of prying the lateral roots out of the soil is very variable and depends on many parameters. Further study of the loss of anchorage in cohesive sediment is advisable to obtain more data points. The influence of the length, thickness and number of the lateral roots on the anchorage and how the forces on these roots are distributed, was beyond the scope of this research.

4.6 Practical implications

First the implication for the WoO framework is discussed in section 4.6.1. Next, the practical implications of the findings of this research for the restoration and creation of salt marshes are considered in section 4.6.2.

4.6.1 Implications for the Windows of Opportunity framework

The research of D. W. Poppema et al. (2019) defined the WoO framework in terms of critical erosion depth as a proxy for erosion instead of bed shear stress proposed by Hu et al. (2015). Poppema argues that using BSS implies that storms are normative, as the highest bed shear stresses are caused by the high waves during storms, while most erosion occurs during moderate events instead of extreme events. Although this reasoning is sound, the WoO2 is defined as a period with calm hydrodynamic conditions and thus, only moderate events can occur in this window and BSS can still be very valuable for the definition of vegetation limits. Moreover, erosion was not the dominant process causing failure in *Salicornia* seedlings growing in cohesive sediment. Therefore this research defines the WoO framework in terms of BSS instead of CED.

The WoO scenarios pertaining the consolidation (Figure 4.5) of cohesive sediment can also give insight into the effect of drought, which reduces the soil moisture content and thus increases consolidation and soil strength. Therefore, when the plants have concluded WoO1, some drought might even be beneficial for the plants. However, persistent drought and the resulting stronger sediment might negatively affect (the next generation of) pioneer plants because of the longer WoO1 window (Figure 4.5 Scenario D). Moreover, this does not take into account other negative aspects of drought on plant growth. For example, an increase of the salinity of porewater and thus salinity stress on the plants and less temperature regulation (Brian, 2007).

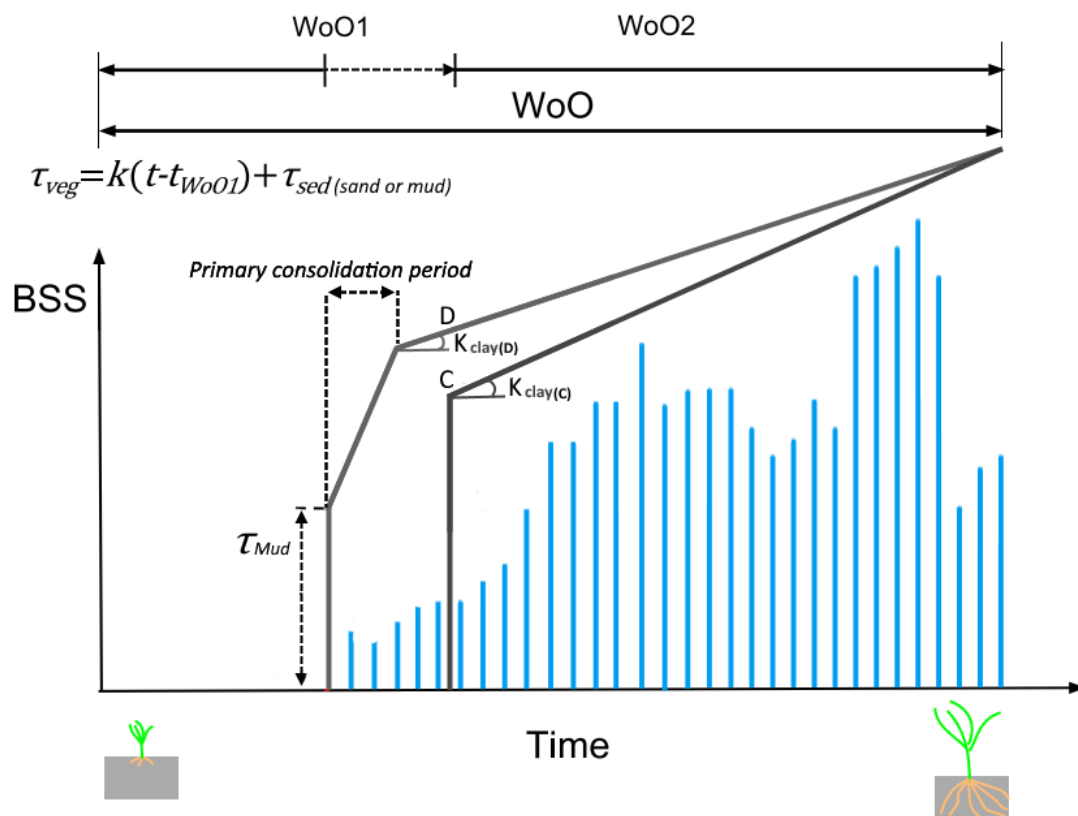


Figure 4.5: Schematization of the WoO adapted from Hu et al., (2015), with different scenarios pertaining consolidation for vegetation establishment in cohesive sediment. Scenario C; consolidation before WoO1 is concluded. Scenario D; consolidation once WoO1 is concluded.

4.6.2 Practical implications for salt marsh restoration and creation

The research of De Vries et al. (2021) and Hendriks (2020) concluded that fine sediment is key for vegetation development and the successful establishment of salt marshes. The research of Hendriks (2020) hypothesized that the positive effect of a high clay percentage on the growth of *Salicornia* could be explained by essential nutrients and high moisture content held in accreted clay. This research seems to confirm this statement; higher clay content in the sediment had a positive effect on the aboveground plant growth of *Salicornia*, especially on the plants' frontal surface area and complexity. Besides supporting the hypothesis of this previous research, this research presents another reason why fine sediments like clay have such a positive effect on pioneer plant establishment on mudflats.

This research demonstrated that juvenile *Salicornia* seedlings in mud could withstand a longer period of wave loading and more wave energy before failure, com-

pared to seedlings of similar age in sand. In clay the seedlings can therefore develop under intenser hydrodynamic conditions and thus colonise a larger part of the intertidal flats. This effect is even more pronounced if the sediment is consolidated once the germinated seedlings are well anchored (after WoO1). *Salicornia* stands facilitate the subsequent establishment of other perennial salt marsh plants; the stands trap vegetative tillers of *Spartina anglica* and *maritima* (van Regteren et al., 2020). These species are key to further increasing the biodiversity and plant succession on a recently established salt marsh, as well as stabilising the soil.

So, a higher clay content may result in a higher survival rate of *Salicornia* seedlings and increase the size of the plants. This results in more trapping of vegetative tillers of perennial salt marsh plants. This can enable these plants to establish in the the regions of the intertidal flats with harsh hydrodynamic conditions, that otherwise would remain barren, and colonise a more considerable portion of the intertidal zone. This is beneficial for ecosystem services like wave attenuation, carbon storage and provides more habitat and marine nursing grounds. Furthermore, a measure to increase consolidation once the WoO1 window has concluded, might increase the successful establishment even further. In practice, there are many different techniques to induce consolidation in the soil. Techniques that are commonly used are preloading and introducing vertical drains to the soil. An alternative technique that is more state of the art, for example electro-osmosis (Bo et al., 2007; Chu et al., 2013). Preloading, although one of the cheaper and well-studied methods may not be the best approach, because the load needs to be applied before the germination of the plants. Consolidation before the conclusion of the WoO1 could hinder further growth. Techniques like installing vertical drains may be a better alternative. The drains can be installed after WoO1, but require a more labour intensive installation processe. Electro-osmosis could be considered, but this technique may not very be cost effective.

Conclusions and recommendations

The aim of this research was “*To determine a set of biophysical parameters and processes underlying the failure of juvenile pioneer salt marsh vegetation, specifically the effect of sediment properties (cohesive and non-cohesive) and wave characteristics, and use these findings improve the understanding of salt marsh plant failure*”. In this section, the two research questions formulated to reach this objective are answered in sections 5.1 and 5.2. In section 5.3 recommendations for future flume experiments are presented.

5.1 Research question 1

- a. *How do plant traits affect the critical erosion depth and failure of *Salicornia procumbens* seedlings?*

The morphology of the roots influences the failure of *Salicornia* seedlings. The root length of the seedlings positively affect the amount of wave loading the seedling can endure. The effect of the aboveground biomass on failure was inconclusive and gave different results in different sediments. Furthermore, the root and shoot length in cohesive sediment were weakly correlated, while in non-cohesive sediment, these plant traits were independent.

- b. *How do sediment properties (cohesive vs. non-cohesive) affect the plant and plant traits over time of *Salicornia procumbens* seedlings?*

Sediment type had a significant impact on the morphology of the seedlings. However, the sediment type had less effect on the aboveground biomass compared to the belowground biomass. The primary difference on the aboveground biomass was plant complexity. The seedlings developing in cohesive sediment grew more complex, with more branches and secondary branches than their counterparts in non-cohesive sediments.

The most crucial difference in plant morphology between sediment types was in the belowground biomass. In non-cohesive sediments, the root system grew wide and complex, with many bifurcations and a lot of surface area. While in cohesive sediment, the root system remained simple and narrow, with a thick primary root and a few primary branches to the side.

- c. *How do sediment properties (cohesive vs. non-cohesive) affect the critical erosion depth and failure of *Salicornia procumbens* seedlings?*

The mechanism of seedling failure is different in cohesive and non-cohesive sediments. In both sediments, the formation of a depression around the plant is responsible for initiating the process of losing root anchorage in the plants. In non-cohesive sediment, erosion is the dominant factor that drives scour-hole formation. This erosion-driven scouring around a plant removes sediment around the roots, which as a result, loses anchorage. Once the scour-hole depth reaches a certain threshold, the critical erosion depth, the roots will not counter the uprooting forces and the plant will flush away completely when submerged.

In cohesive sediments, erosion is only a minor factor in the formation of a depression around a plant. Instead, the to-and-fro motion of the plants and the deformation of the sediment around the plants drive the depression formation around a plant. This deformation cavity allows for progressively more movement space around the seedlings and this will put more stress on the lateral roots keeping the plant upright. Once a certain threshold is reached, these lateral roots will break or fail because of the to-and-fro motion and the plant will not be able to remain upright when unsubmerged. Because erosion was not the main driver for the failure of *Salicornia* seedlings in cohesive sediment, the critical erosion depth was less relevant.

During the flume experiment, plants growing in cohesive sediment could endure, on average more time under wave loading, compared to plants growing in non-cohesive sediment before failure. Furthermore, the scour-holes in non-cohesive were on average 2.5 times deeper than the holes cohesive sediment.

- d. *How do irregular wave characteristics affect the critical erosion depth and failure of *Salicornia procumbens* seedlings?*

Irregular waves produced periods of high flow velocity and periods in which the flow velocity was moderate. This translated to the BSS and plant motion produced by these oscillating flows. These periods of high BSS peaks with extended plant motion stressed the plant roots in cohesive and non-cohesive sediment.

Over time, this reduced the anchorage of the seedlings and eventually led to failure. During periods with moderate flow velocities, the BSS could only cause some sediment transport in the non-cohesive sediment and the plant motion was limited.

Because of morphological differences between seedlings in cohesive and non-cohesive sediment, a typical plant in cohesive sediment received more wave energy over time compared to a seedling in non-cohesive sediment.

5.2 Research question 2

- a. *How can the observations of the flume experiment be used to improve the Windows of Opportunity framework for salt marsh establishment?*

The observations of the flume experiment were used to formulate distinct scenarios for the Windows of Opportunity framework, for different sediment properties. In cohesive sediment, erosion was not the dominant process that induced failure in *Salicornia* seedlings. So instead of critical erosion depth, in this research the Windows of Opportunity framework was defined in terms of bed shear stress. Sediment properties also influenced the amount of wave loading a seedling could endure. Seedlings growing in cohesive sediment could withstand more wave loading compared to seedlings of similar age in non-cohesive sediment. Thus, the WoO2 for seedlings growing in cohesive sediment is more flexible than the WoO2 of seedlings growing in non-cohesive sediment. This is even more pronounced when the cohesive sediment is consolidated with high soil strength. Sediment consolidation also affects the WoO1; slower root elongation and reduced root length were observed in consolidated clay. Therefore, consolidation before the conclusion of the WoO1 window can extend the duration of the window. So, in this research the WoO framework has been improved by adding sediment properties to this salt marsh establishment concept.

- b. *What are the practical implications of the observations of the flume experiment for restoration of salt marshes*

This research demonstrated that sediment properties affect the failure of *Salicornia* seedlings; a higher clay content may result in a higher survival rate of *Salicornia* seedlings and increase the frontal surface area of the plants. This can enable perennial salt marsh plants to establish on the intertidal flats, particularly the zones with harsher hydrodynamic conditions. Furthermore, a measure to increase consolidation once the seedlings have sufficient root anchorage, might increase the successful establishment even further. So, the increased survival

rate of *Salicornia* in cohesive sediments can aid the expansion and succession of a salt marsh. This is beneficial for ecosystem services like wave attenuation, carbon storage and provides more habitat and marine nursing grounds.

5.3 Recommendations for future flume experiments

This research suggests that artificially grown plants perform well under wave loading. However, artificially grown plants that are not exposed to tides or periodic wave loading might be disadvantaged once introduced to wave loading. During the experiment, we observed that the plants could withstand the forces produced by waves well; the artificially grown plants can therefore be a good proxy for field plants for future experiments in the wave flume .

Testing field samples is very relevant to study the practical implications of the research. During the flume experiment however, the field samples failed in the flume because the original sediment did not cohere well with the sediment in the boxes. A solution would be to take a whole slab of sediment from the field in which the plants grew and shape this to the boxes so all the sediment in a box is coherent.

For future flume experiments, it might be beneficial to devise a way to measure the exact moment of failure. During the experiment, we tried to accomplish this by using an Ultrasonic High Concentration Meter (UHCM)) measurement device, but this did not work. Due to high turbidity in the flume after a few runs, visual determination of failure also proved to be difficult. Furthermore, this study focused primarily on irregular waves; for future experiments, it might be beneficial to include tests with regular waves to study the effect of these types of waves under comparable conditions as the irregular waves.

Bibliography

- Adam, P. (2018). *Salt marsh restoration*. <https://doi.org/10.1016/B978-0-444-63893-9.00023-X>
- Balke, T. (2013). *Establishment of biogomorphic ecosystems*.
- Balke, T., Bouma, T. J., Horstman, E. M., Webb, E. L., Erftemeijer, P. L., & Herman, P. M. (2011). Windows of opportunity: Thresholds to mangrove seedling establishment on tidal flats. *Marine Ecology Progress Series*, 440(May 2014), 1–9. <https://doi.org/10.3354/meps09364>
- Beeftink, W. G. (1985). Population dynamics of annual *Salicornia* species in the tidal salt marshes of the Oosterschelde, The Netherlands. *Vegetatio*, 61(1-3), 127–136. <https://doi.org/10.1007/BF00039817>
- Bengough, A. G., Bransby, M. F., Hans, J., McKenna, S. J., Roberts, T. J., & Valentine, T. A. (2006). Root responses to soil physical conditions; growth dynamics from field to cell. *Journal of Experimental Botany*, 57(2 SPEC. ISS.), 437–447. <https://doi.org/10.1093/jxb/erj003>
- Bo, M. W., Arulrajah, A., & Nikraz, H. (2007). Preloading and prefabricated vertical drains design for foreshore land reclamation projects: A case study. *Ground Improvement*, 11(2), 67–76. <https://doi.org/10.1680/grim.2007.11.2.67>
- Bouma, T. J., Friedrichs, M., Klaassen, P., Van Wesenbeeck, B. K., Brun, F. G., Temmerman, S., Van Katwijk, M. M., Graf, G., & Herman, P. M. (2009). Effects of shoot stiffness, shoot size and current velocity on scouring sediment from around seedlings and propagules. *Marine Ecology Progress Series*, 388(May 2014), 293–297. <https://doi.org/10.3354/meps08130>
- Bouma, T. J., Temmerman, S., van Duren, L. A., Martini, E., Vandenbruwaene, W., Callaghan, D. P., Balke, T., Biermans, G., Klaassen, P. C., van Steeg, P., Dekker, F., van de Koppel, J., de Vries, M. B., & Herman, P. M. (2013). Organism traits determine the strength of scale-dependent bio-geomorphic feedbacks: A flume study on three intertidal plant species. *Geomorphology*, 180-181, 57–65. <https://doi.org/10.1016/j.geomorph.2012.09.005>
- Bouma, T. J., van Belzen, J., Balke, T., van Dalen, J., Klaassen, P., Hartog, A. M., Callaghan, D. P., Hu, Z., Stive, M. J., Temmerman, S., & Herman, P. M. (2016). Short-term mudflat dynamics drive long-term cyclic salt marsh dy-

- namics. *Limnology and Oceanography*, 61(6), 2261–2275. <https://doi.org/10.1002/lno.10374>
- Bradley, P., & Morris, J. (1990). Physical characteristics of salt marsh sediments: ecological implications. *Marine Ecology Progress Series*, 61, 245–252. <https://doi.org/10.3354/meps061245>
- Callaghan, D. P., Bouma, T. J., Klaassen, P., van der Wal, D., Stive, M. J., & Herman, P. M. (2010). Hydrodynamic forcing on salt-marsh development: Distinguishing the relative importance of waves and tidal flows. *Estuarine, Coastal and Shelf Science*, 89(1), 73–88. <https://doi.org/10.1016/j.ecss.2010.05.013>
- Cao, H., Zhu, Z., Balke, T., Zhang, L., & Bouma, T. J. (2018). Effects of sediment disturbance regimes on *Spartina* seedling establishment: Implications for salt marsh creation and restoration. *Limnology and Oceanography*, 63(2), 647–659. <https://doi.org/10.1002/lno.10657>
- Cao, H., Zhu, Z., James, R., Herman, P. M. J., Zhang, L., Yuan, L., & Bouma, T. J. (2019). Wave effects on seedling establishment of three pioneer marsh species : survival , morphology and biomechanics, 1–8. <https://doi.org/10.1093/aob/mcz136>
- Chen, H., Ni, Y., Li, Y., Liu, F., Ou, S., Su, M., Peng, Y., Hu, Z., Uijtewaal, W., & Suzuki, T. (2018). Deriving vegetation drag coefficients in combined wave-current flows by calibration and direct measurement methods. *Advances in Water Resources*, 122, 217–227. <https://doi.org/10.1016/j.advwatres.2018.10.008>
- Chu, J., Indraratna, B., Yan, S., & Rujikiatkamjorn, C. (2013). *Soft Soil Improvement Through Consolidation: An Overview*. https://doi.org/10.3850/978-981-07-3559-3{_}103-0007
- Church, J. A., & Gregory, J. M. (2019). Sea level change. *Encyclopedia of Ocean Sciences*, 493–499. <https://doi.org/10.1016/B978-0-12-409548-9.10820-6>
- Davy, A. J., Bishop, G. F., & Costa, C. S. (2001). *Salicornia* L. (*Salicornia pusilla* J. Woods, *S. ramosissima* J. Woods, *S. europaea* L., *S. obscura* P.W. Ball & Tutin, *S. nitens* P.W. Ball & Tutin, *S. fragilis* P.W. Ball & Tutin and *S. dolichostachya* Moss). *Journal of Ecology*, 89(4), 681–707. <https://doi.org/10.1046/j.0022-0477.2001.00607.x>
- De Vries, B., Willemsen, P., Van Puijenbroek, L., M.E.B. Coumou, Baptist, M., Clev-eringa, J., Dankers, P., & Elschot, K. (2021). Salt marsh pilot Marconi; monitoring results, 88. https://www.ecoshape.org/app/uploads/sites/2/2016/07/MarconiSaltmarsh_ReportAnalysisSaltmarshDevelopment_220121_def.pdf
- Denny, M., Helmuth, B., & Daniel, T. (1998). The menace of momentum : Dynamic forces on flexible organisms. 43(5), 955–968.

- Edmaier, K., Burlando, P., & Perona, P. (2011). Mechanisms of vegetation uprooting by flow in alluvial non-cohesive sediment. *Hydrology and Earth System Sciences*, 15(5), 1615–1627. <https://doi.org/10.5194/hess-15-1615-2011>
- Faber, P. W., & Phyllis. (2001). Salt Marsh Restoration Experience in San Francisco Bay. *Journal of Coastal Research*, 27, 203–211.
- Friess, D. A., Krauss, K. W., Horstman, E. M., Balke, T., Bouma, T. J., Galli, D., & Webb, E. L. (2012). Are all intertidal wetlands naturally created equal? Bottlenecks, thresholds and knowledge gaps to mangrove and saltmarsh ecosystems. *Biological Reviews*, 87(2), 346–366. <https://doi.org/10.1111/j.1469-185X.2011.00198.x>
- Gedan, K. B., Silliman, B. R., & Bertness, M. D. (2009). Centuries of human-driven change in salt marsh ecosystems. *Annual Review of Marine Science*, 1(May 2014), 117–141. <https://doi.org/10.1146/annurev.marine.010908.163930>
- Germaine, J. T., Madsen, O. S., Ladd, C. C., & Member, H. (1998). EROSIONAL AND MECHANICAL STRENGTHS OF DEPOSITED. 124(11), 1076–1085.
- Gillen, M., Messerschmidt, T., & Kirwan, M. (2020). Biophysical Controls of Marsh Soil Shear Strength Along an Estuarine Salinity Gradient. (July), 1–15. <https://doi.org/10.1130/abs/2020se-342719>
- Hendriks, M. E. (2020). effect of seeding and sediment composition on pioneer species *Salicornia*.
- Houwing, E. J. (1999). Determination of the Critical Erosion Threshold of Cohesive Sediments on Intertidal Mudflats Along the, 545–555.
- Houwing, E. J. (2000). Morphodynamic development of intertidal mudflats: Consequences for the extension of the pioneer zone. *Continental Shelf Research*, 20(12-13), 1735–1748. [https://doi.org/10.1016/S0278-4343\(00\)00045-5](https://doi.org/10.1016/S0278-4343(00)00045-5)
- Hu, Z., Van Belzen, J., Van Der Wal, D., Balke, T., Wang, Z. B., Stive, M., & Bouma, T. J. (2015). Windows of opportunity for salt marsh vegetation establishment on bare tidal flats: The importance of temporal and spatial variability in hydrodynamic forcing. *Journal of Geophysical Research G: Biogeosciences*, 120(7), 1450–1469. <https://doi.org/10.1002/2014JG002870>
- Jacobs, W. (2011). *Sand-mud erosion from a soil mechanical perspective Proefschrift ter*.
- Jadhav, R. S., Chen, Q., & Smith, J. M. (2013). Spectral distribution of wave energy dissipation by salt marsh vegetation. 77, 99–107. <https://doi.org/10.1016/j.coastaleng.2013.02.013>
- JRC PESETA II project. (2009). Climate change and coastal floods.
- Khan, F. S., Azam, S., Raghunandan, M. E., & Clark, R. (2014). Compressive strength of compacted clay-sand mixes. *Advances in Materials Science and Engineering*, 2014. <https://doi.org/10.1155/2014/921815>

- Kothyari, U., Kumar, A., & Jain, R. (2014). Influence of Cohesion on River Bed Scour in the Wake Region of Piers. *Journal of Hydraulic Engineering*, 140(1), 1–13. [https://doi.org/10.1061/\(asce\)hy.1943-7900.0000793](https://doi.org/10.1061/(asce)hy.1943-7900.0000793)
- Kranenburg, C., & Winterwerp, J. C. (1997). Erosion of Fluid Mud Layers. I: Entrainment Model. *Journal of Hydraulic Engineering*, 123(6), 504–511. [https://doi.org/10.1061/\(asce\)0733-9429\(1997\)123:6\(504\)](https://doi.org/10.1061/(asce)0733-9429(1997)123:6(504))
- Leonardi, N., & Fagherazzi, S. (2015). Effect of local variability in erosional resistance on large-scale morphodynamic response of salt marshes to wind waves and extreme events, 5872–5879. <https://doi.org/10.1002/2015GL064730>. Received
- Lo, V. B., Lo, V. B., Bouma, T. J., Belzen, J. V., Colen, C. V., & Airoldi, L. (2017). Interactive effects of vegetation and sediment properties on erosion of salt marshes in the Northern Adriatic Sea Marine Environmental Research Interactive effects of vegetation and sediment properties on erosion of salt marshes in the Northern Adriatic S. (September). <https://doi.org/10.1016/j.marenvres.2017.09.006>
- McClave, J. T., Benson, G. P., Sincich, T., & Knypstra, S. (2011). *Statistiek, een inleiding* (Elfde edit). Pearson.
- Mickovski, S. B. (2003). ANCHORAGE MECHANICS OF DIFFERENT TYPES OF ROOT SYSTEMS To cite this version : HAL Id : tel-00003454.
- Mitsch, W., & Gosselink, J. (2007). *Wetlands*. John Wiley & Sons, inc.
- Mohan, R. K., Conshohocken, W., Finkl, C. W., & Makowski, C. (2019). *Encyclopedia of Coastal Science: Capping of Contaminated Coastal*.
- Möller, I., Kudella, M., Rupprecht, F., Spencer, T., Paul, M., Wesenbeeck, B. K. V., Wolters, G., Jensen, K., Bouma, T. J., Miranda-lange, M., & Schimmels, S. (2014). Wave attenuation over coastal salt marshes under storm surge conditions. 7(September), 727–732. <https://doi.org/10.1038/NGEO2251>
- Nepf, H. M. (2012). *Flow Over and Through Biota* (Vol. 2). <https://doi.org/10.1016/B978-0-12-374711-2.00213-8>
- Nicholls, R. J., Hoozemans, F. M., & Marchand, M. (1999). Increasing flood risk and wetland losses due to global sea-level rise: Regional and global analyses. *Global Environmental Change*, 9(SUPPL.). [https://doi.org/10.1016/S0959-3780\(99\)00019-9](https://doi.org/10.1016/S0959-3780(99)00019-9)
- Nottage, A., & Robertson, P. (2005). *The saltmarsh creation handbook : a project manager's guide to the creation of saltmarsh and intertidal mudflat*.
- Onorato, M., Osborne, A. R., Serio, M., Cavaleri, L., Brandini, C., & Stansberg, C. T. (2006). Extreme waves, modulational instability and second order theory: wave flume experiments on irregular waves. *European Journal of Mechanics, B/Fluids*, 25(5), 586–601. <https://doi.org/10.1016/j.euromechflu.2006.01.002>

- Perera, C., Smith, J., Wu, W., Perkey, D., & Priestas, A. (2020). Erosion rate of sand and mud mixtures. *International Journal of Sediment Research*, 35(6), 563–575. <https://doi.org/10.1016/j.ijsrc.2020.06.004>
- Poppema, D. (2017). Experiment - supported modelling of salt marsh establishment : Applying the Windows of opportunity. (June), 68.
- Poppema, D. W., Willemsen, P. W., de Vries, M. B., Zhu, Z., Borsje, B. W., & Hulscher, S. J. (2019). Experiment-supported modelling of salt marsh establishment. *Ocean and Coastal Management*, 168(September 2018), 238–250. <https://doi.org/10.1016/j.ocecoaman.2018.10.039>
- Rozas, L. P., Caldwell, P., Minello, T. J., Rozasf, L. P., Caldwell, P., & Minello, T. J. (2016). The Fishery Value of Salt Marsh Restoration Projects Stable URL : <http://www.jstor.org/stable/25736614> Linked references are available on JSTOR for this article : The Fishery Value of Salt Marsh Restoration Projects. (40), 37–50.
- Schoutens, K., Reents, S., Nolte, S., Evans, B., Paul, M., Kudella, M., Bouma, T., Möller, I., & Temmerman, S. (2021). Survival of the thickest? Impacts of extreme wave-forcing on marsh seedlings are mediated by species morphology. *Limnology and Oceanography*, (1), 1–16. <https://doi.org/10.1002/lno.11850>
- Schroever, M., Huisman, B. J. A., Wal, M. V. D., & Nortek, B. V. (2010). Measuring ship induced waves and currents on a tidal flat in the Western Scheldt Estuary. *2011 IEEE/OES 10th Current, Waves and Turbulence Measurements (CWTM)*, 123–129. <https://doi.org/10.1109/CWTM.2011.5759539>
- Schutten, J., Dainty, J., & Davy, A. J. (2005). Root anchorage and its significance for submerged plants in shallow lakes. *Journal of Ecology*, 93(3), 556–571. <https://doi.org/10.1111/j.1365-2745.2005.00980.x>
- Silinski, A., Heuner, M., Troch, P., Puijalón, S., Bouma, T. J., Schoelynck, J., Schröder, U., Fuchs, E., Meire, P., & Temmerman, S. (2016). Effects of contrasting wave conditions on scour and drag on pioneer tidal marsh plants. *Geomorphology*, 255, 49–62. <https://doi.org/10.1016/j.geomorph.2015.11.021>
- Soulsby, R. (1997). *Dynamics of marine sands: A manual for practical applications*. Thomas Telford Publications.
- Spencer, T., Möller, I., Rupprecht, F., Bouma, T. J., van Wesenbeeck, B. K., Kudella, M., Paul, M., Jensen, K., Wolters, G., Miranda-Lange, M., & Schimmels, S. (2016). Salt marsh surface survives true-to-scale simulated storm surges. *Earth Surface Processes and Landforms*, 41(4), 543–552. <https://doi.org/10.1002/esp.3867>
- Sun, Z., Mou, X., Lin, G., Wang, L., Song, H., & Jiang, H. (2010). Effects of sediment burial disturbance on seedling survival and growth of *Suaeda salsa* in the

- tidal wetland of the Yellow River estuary. *Plant and Soil*, 337(1), 457–468. <https://doi.org/10.1007/s11104-010-0542-8>
- Townend, I., Fletcher, C., Knappen, M., & Rossington, K. (2011). A review of salt marsh dynamics. *Water and Environment Journal*, 25(4), 477–488. <https://doi.org/10.1111/j.1747-6593.2010.00243.x>
- van der Wal, D., & Herman, P. M. (2012). Ecosystem Engineering Effects of *Aster tripolium* and *Salicornia procumbens* Salt Marsh on Macrofaunal Community Structure. *Estuaries and Coasts*, 35(3), 714–726. <https://doi.org/10.1007/s12237-011-9465-8>
- Van Rijn, L. C., Nieuwjaar, M. W. C., van der Kaay, T., Nap, E., & van Kampen, A. (1993). Transport of Fine Sands by Currents and Waves. *Journal of Waterway, Port, Coastal, and Ocean Engineering*, 119(2), 123–143. [https://doi.org/10.1061/\(asce\)0733-950x\(1993\)119:2\(123\)](https://doi.org/10.1061/(asce)0733-950x(1993)119:2(123))
- van Regteren, M., Meesters, E. H., Baptist, M. J., de Groot, A. V., Bouma, T. J., & Elschot, K. (2020). Multiple Environmental Variables Affect Germination and Mortality of an Annual Salt Marsh Pioneer: *Salicornia procumbens*. *Estuaries and Coasts*, 43(6), 1489–1501. <https://doi.org/10.1007/s12237-020-00735-y>
- van Rijn, L. C., & Barth, R. (2018). SETTLING AND CONSOLIDATION OF SOFT MUD-SAND LAYERS. in *Journal of Waterway, Port, Coastal and Ocean Engineering*.
- Wang, W., Luo, Q., Yuan, B., & Chen, X. (2020). An Investigation of Time-Dependent Deformation Characteristics of Soft Dredger Fill. *Advances in Civil Engineering*, 2020. <https://doi.org/10.1155/2020/8861260>
- Willemsen, P. W., Borsje, B. W., Hulscher, S. J., Van der Wal, D., Zhu, Z., Oteman, B., Evans, B., Möller, I., & Bouma, T. J. (2018). Quantifying Bed Level Change at the Transition of Tidal Flat and Salt Marsh: Can We Understand the Lateral Location of the Marsh Edge? *Journal of Geophysical Research: Earth Surface*, 123(10), 2509–2524. <https://doi.org/10.1029/2018JF004742>
- William, C. M., Charles W. Finkl. (2019). *Encyclopedia of Coastal Science*.
- Wolters, M., Garbutt, A., & Bakker, J. P. (2005). Salt-marsh restoration: Evaluating the success of de-embankments in north-west Europe. *Biological Conservation*, 123(2), 249–268. <https://doi.org/10.1016/j.biocon.2004.11.013>
- Yeager, K. M., Baird, A. H., Feagin, R. A., Ravens, T. M., & Mo, I. (2009). Does vegetation prevent wave erosion of salt marsh edges ? *106(25)*, 10109–10113.
- You, Z., Yin, B., & Huo, G. (2009). Direct measurement of wave-induced bottom shear stress under irregular waves. *Advances in Water Resources and Hydraulic Engineering - Proceedings of 16th IAHR-APD Congress and 3rd Symposium of IAHR-ISHS*, 1213–1218. https://doi.org/10.1007/978-3-540-89465-0_{_}211

- Young, I. R. (2017). Regular, Irregular Waves and the Wave Spectrum. *Encyclopedia of Maritime and Offshore Engineering*, (April), 1–10. <https://doi.org/10.1002/9781118476406.emoe078>

Appendix A

Drag coefficients in different flow regimes

Study	Re_d	Flow	C_D - Drag coefficient
Armanini et al. 2005* willow, d = trunk diameter	5000 to 20000	current	1.5 with foliage 1 without foliage
Mazda et al* Mangrove forest (field), Re length-scale is a^{-1} instead of d	2000 to 90000	tidal current	0.4 to 10, increasing as Re_d decreases
Ghisalberti & Nepf 2006 ** <i>Zostera marina</i> flexible model	30 to 100	current	1 ± 0.1
Ghisalberti & Nepf 2006 * rigid cylinder array	80 to 400	current	0.7 ± 0.1
Ciraolo et al. 2006** <i>Posidonia oceanica</i> flexible model	40 to 700	current	$O(1)$ for $Re_d > 200$ 1-10 for $Re_d < 200$ increasing as Re_d decreases
Wilson et al. 2008** pine and ivy stems	$U =$ 25 to 60 cms^{-1}	current	pine with foliage, 0.5 to 1.1, \downarrow with $\uparrow U$ pine w/o foliage, 0.5 to 1.3, $\neq f(U)$ ivy with foliage, 0.5 to 0.8, \downarrow with $\uparrow U$ ivy w/o foliage, 0.5 to 3.3, $\neq f(U)$,
Kobayashi et al. 1993* flexible plastic strips C_D assumes strips are rigid	2000 to 16000	waves	$O(0.1)$ for $Re_d > 8000$ $C_D = 0.08 + (2200/Re_d)^{2.4}$
Mendez et al. 1999 * flexible plastic strips C_D accounts for plant motion	2000 - 16000	waves	$O(0.4)$ for $Re_d > 8000$ $C_D = 0.4 + (4600/Re_d)^{2.9}$
Bradley & Houser 2009* Seagrass, <i>Thalassia testudinum</i> (field) C_D accounts for plant motion	200 to 800	waves	1 to 100, increasing as Re_d decreases $C_D = (925/Re_d)^{3.5}$
McDonald et al. 2006* Coral, <i>Porites compressa</i>	$U = 1$ to 25 cms^{-1}	current	$C_D = 1.01 (H/h)^{-2.8} + 0.01$ H = water depth, h = coral height
Lowe et al 2008* Coral, <i>Porites compressa</i>	$U_{\infty} = 11 \text{ cms}^{-1}$ $U_{\text{rms}} = 5 \text{ cms}^{-1}$	current waves	$\beta = 19$ to 27 m^{-1} (eq. 13b) $\beta = 4$ to 6 m^{-1} (eq. 13b) variation reflects different coral configurations

Table 1
A review of C_D relations in vegetation-wave interaction and their deriving methods.

Reference	Mimic Type	Flow condition	C_D relation	Deriving method
Kobayashi et al. (1993)	Flexible plastic strips	Waves	$C_D = 0.08 + (2200/Re)^{2.4}$ $2200 < Re < 18,000$	Calibration method
Méndez et al. (1999)	Flexible plastic strips	Waves	$C_D = 0.08 + (2200/Re)^{2.2}$ $2000 < Re < 15,500$ (no swaying) $C_D = 0.40 + (4600/Re)^{2.9}$ $2300 < Re < 20,000$ (swaying)	Calibration method
Mendez and Losada (2004)	Flexible real vegetation	Waves	$C_D = 0.47 \exp(-0.052KC)$ $R^2 = 0.76$ $3 \leq KC \leq 59$	Calibration method
Bradley and Houser (2009)	Flexible real vegetation	Waves	$C_D = 253.9KC^{-3.0}$ $R^2 = 0.95$ $0 < KC < 6$ Field data Calculated using the relative velocity of the seagrass blades	Calibration method
Ranjit S. Jadhav et al. (2013)	Flexible real vegetation	Waves	$C_D = 70KC^{-0.86}$ $R^2 = 0.95$ $25 < KC < 135$	Calibration method
Anderson and Smith (2014)	Flexible plastic strips	Waves	$C_D = 1.10 + (27.4/KC)^{3.08}$ $R^2 = 0.88$ $26 < KC < 112$ $C_D = 0.76 + (744.2/Re)^{1.27}$ $R^2 = 0.94$	Calibration method
Ozeren et al. (2014) ^b	Rigid wooden cylinders	Waves	$C_D = 1.5 + (6.785/KC)^{2.22}$ $R^2 = 0.21$ $N_s = 156m^{-2}$, $h_s = 0.63m$ $C_D = 2.1 + (793/Re)^{2.39}$	Calibration method
	Flexible plastic strips		$C_D = 0.683 + (12.07/KC)^{2.25}$ $N_s = 350m^{-2}$, $h_s = 0.48m$	
Infantes et al. (2011)	Flexible real vegetation	Waves	$\lg C_D = -0.6653 \lg Re + 1.1886$ $R^2 = 0.77$	Direct measurement method
Hu et al. (2014)	Rigid wooden cylinders	Wave + Current	$C_D = 1.04 + (730/Re)^{1.37}$ $R^2 = 0.66$ $300 < Re < 4700$	Direct measurement method
Losada et al. (2016a,b)	Flexible real vegetation	Wave \pm Current	$C_D = 0.08 + (50,000/Re)^{2.2}$ $R^2 = 0.60$ (regular waves) $C_D = 0.25 + (75,000/Re)^9$ (regular waves + currents) $C_D = 0.50 + (50,000/Re)^9$ (regular waves-currents)	Calibration method

Appendix B

Flow velocity field

This research compares the irregular wave spectrum produced in the flume experiment to a monochromatic wave spectrum with comparable wave characteristics (e.g., wave height, water depth and period). Using linear wave theory (Newman, 2017; R. L. Soulsby, 1987) the flow velocities produced by such a monochromatic wave are determined in Matlab. The velocity field can be calculated using equation B.1

$$u = A\omega \frac{\cosh k(y+h)}{\sinh kh} * \cos(kx - \omega t) \quad (\text{B.1})$$

$$A = \frac{H}{2} \quad (\text{B.2})$$

$$\omega = \frac{2\pi}{T} \quad (\text{B.3})$$

$$kh \approx \sqrt{C}(1 + 0.169C + 0.031C^2 + \dots) \quad (\text{B.4})$$

$$C = \omega^2 \frac{h}{g} \quad (\text{B.5})$$

Appendix C

Calculation of species-specific attachment coefficient (k)

$$k = \frac{F_a}{A_r^{\frac{2}{3}} * C_u} \quad (C.1)$$

Using sample 23

$$9.69 = \frac{300}{0.0000468^{\frac{2}{3}} * 23850} \quad (C.2)$$

sample	F removal (g)	Area root system (cm^2)	Area root system (m^2)	Soil length (Pa)	k
11	430	1	0.0001	14230	14.026
13	40	1.2	0.00012	23850	0.69
21	150	0.79	0.000079	12730	6.40
23	300	0.468	0.0000468	23850	9.69
34	110	0.5237	0.00005237	10800	7.28
19	65	0.87	0.000087	39450	0.84

Average value for k=6.48